The role of fault zones and melts as agents of weakening, hardening and differentiation of the continental crust: a synthesis

M.R. HANDY[1], A. MULCH[1,2], M. ROSENAU[1,3] & C.L. ROSENBERG[1]

[1]*Freie Universität Berlin, Geowissenschaften, Malteserstrasse 74–100, Haus B, Geologie, D-12249 Berlin, Germany (e-mail: mhandy@zedat.fu-berlin.de)*

[2]*Present address: Université de Lausanne, Institut de Minéralogie et Pétrographie, BFSH 2, CH-1015 Lausanne, Switzerland*

[3]*Present address: Geoforschungszentrum Potsdam, Haus C, D-14473 Potsdam, Germany*

Abstract: The rheology of crustal fault zones containing melts is governed primarily by two strain-dependent mechanical discontinuities: (1) a strength minimum parallel to mylonitic foliation just below the active brittle–viscous (b–v) transition; (2) the anatectic front, which marks the upper depth limit of anatectic flow. The mode of syntectonic melt segregation in fault zones is determined by the scale of strain localization and melt-space connectivity, to an extent dependent on strain, strain rate and melt fraction in the rock. Melt drains from the mylonitic wall rock into dilatant shear surfaces, which propagate sporadically as veins. Anatectic flow at natural strain rates therefore involves melt-assisted creep punctuated by melt-induced veining. On the crustal scale, dilatant shear surfaces and vein networks serve as conduits for the rapid, buoyancy-driven ascent of transiently overpressured melt from melt-source rocks at or just below the anatectic front to sinks higher in the crust. Strength estimates for natural rocks that experienced anatectic flow indicate that melts weaken the continental crust, particularly in depth intervals where they spread laterally beneath low-permeability layers or along active shear zones with a pronounced mylonitic foliation. However, acute weakening associated with strength drops of more than an order of magnitude occurs only during short periods (10^3–10^5 a) of crustal-scale veining. Cooling and crystallization at the end of these veining episodes is fast and hardens the crust to strengths at least as great as, and in some cases greater than, its pre-melting strength. Repeated melt-induced weakening then hardening of fault zones may be linked to other orogenic processes that occur episodically (shifting centres of clastic sedimentation and volcanism) and has implications for stress transmission across orogenic wedges and magmatic arcs.

Molten rock originates and accumulates at structurally controlled sites within the continental crust in a wide range of tectonic settings, as documented in a growing literature on melt-related tectonics (for examples and references, see Fig. 1). Melting is a harbinger of nascent plate boundaries, as well as a process at active and formerly active, divergent, convergent and transcurrent boundaries (Prichard *et al.* 1993 and papers therein). Although there is broad consensus that melting is spatially and temporally related to crustal-scale fault zones (Hollister & Crawford 1986; Speer *et al.* 1994; Vigneresse 1995) on at least some scales of observation (Paterson & Schmidt 1999), the causes and processes underlying this close relationship remain controversial.

Debate has centred on the question of whether melting causes strain localization or vica versa. Melts either deform rock by forcing their way and creating space (Hutton 1988*a*; Paterson *et al.* 1989; De Saint Blaquat *et al.* 1998), or fill space opened by incompatible rock deformation on both the local (Collins & Sawyer 1996) and regional scales (e.g. Hutton 1988a). This chicken-or-egg-first dilemma has been apparently resolved by the insight that melting and deformation are linked in a positive feedback loop (Brown & Solar 1998) such that melt-enhanced strain localization leads to further melt segregation (Brown 1994) and crustal differentiation. We will have more to say about this below, but point out that the main problem underlying debates on melt transport and emplacement is our limited knowledge of the deformation mechanisms and rheology of partially melted rock at high strains.

From: HOLDSWORTH, R.E., STRACHAN, R.A., MAGLOUGHLIN, J.F. & KNIPE, R.J. (eds) 2001. *The Nature and Tectonic Significance of Fault Zone Weakening*. Geological Society, London, Special Publications, **186**, 305–332. 0305-8719/01/$15.00

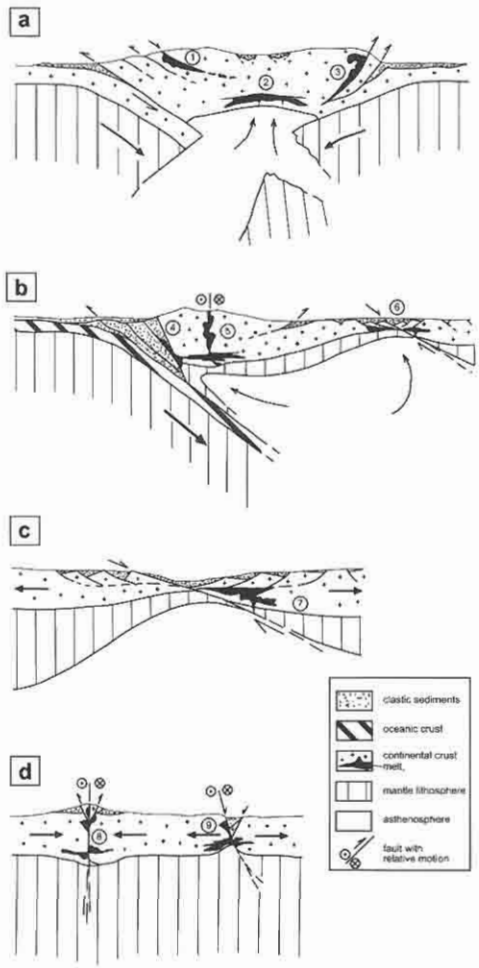

Fig. 1. Phanerozoic tectonic settings of fault-related melt transport and emplacement. Circled letters correspond to settings and references numbered sequentially below. (**a**) Collisional orogens: (1) granitic rocks in footwall of synorogenic extensional faults, e.g. Tertiary leucogranites beneath North Himalayan Normal Fault (Burg *et al.* 1984; England & Molnar 1993); (2) melts beneath high intramontane plateaux, e.g. Tibetan plateau north of the Himalaya (Nelson *et al.* 1996), Altiplano–Puna plateau in the Central Andes (Scheuber & Reutter 1992; Allmendinger *et al.* 1997); (3) intrusive rocks along late-orogenic backthrusts bounding the retro-wedge of orogens, e.g. Tertiary intrusive rocks along the Periadriatic (Insubric) Line bordering the Central Alps (Dietrich 1976; Rosenberg *et al.* 1995; von Blanckenburg & Davies 1995; Davidson *et al.* 1996), Late Cretaceous–Early Tertiary tonalite along Valdez Creek Shear Zone bordering the MacLaren Glacier metamorphic belt, south–central Alaska (Hollister & Crawford 1986; Davidson *et al.* 1992). (**b**) Magmatic arcs: (4) forearc intrusive rocks, e.g. Tertiary S-type granites in forearc, Eastern Gulf of Alaska (Barker *et al.* 1992); (5) transpressional strike-slip systems between forearcs and back-arcs, e.g. Great Sumatran and Mentawi Faults (De Saint Blaquat *et al.* 1998); (6) footwall of uniform-sense, back-arc extensional shear zones, e.g. Tertiary granitic rocks beneath low-angle normal faults, northern Tyrrhenian Sea (e.g. Daniel & Jolivet 1995), Aegean Sea (Lister & Baldwin 1993). (**c**) Continental rifts: (7) granites in footwall of low-angle normal faults, e.g. Cordilleran metamorphic core complexes (Crittenden *et al.* 1980), basic melts beneath Tertiary to Recent Basin-and-Range and Rio Grande rift systems (Olsen *et al.* 1987), Tertiary East African rift system (Bailey 1992). (**d**) Continental transforms: (8) calc-alkaline intrusive rocks within transpressive shear zones, e.g. Cadomian North Armorican Shear Zone (D'Lemos *et al.* 1992), Late Palaeozoic South Armorican Shear Zone (Gapais 1989; Vigneresse 1995), Devonian Central Main Belt shear zone, northern Appalachians (Brown & Solar 1998, Brown & Solar 1999), Ox Mountains igneous complex (McCaffrey 1992); (9) calc-alkaline intrusive rocks within transtensional shear zones, e.g. Early Permian Cossato–Mergozzo–Brissago Line in Ivrea–Verbano Zone, Southern European Alps (Handy & Streit 1999, and this paper), gabbroic melts beneath Salton Trough, Gulf of California (Lachenbruch *et al.* 1985), Main Donegal Granite, NW Ireland (Hutton 1982), granites along transtensional splay of Great Glen Fault, Scotland (Hutton 1988b).

The fact that some melt-bearing shear zones accommodated large displacements (greater than tens of kilometres) suggested long ago that melts may enhance strain localization and facilitate rapid exhumation of the continental crust (e.g. Hollister & Crawford 1986). This inference is apparently consistent with experiments showing that silicic melt viscosities are many orders of magnitude lower than those of crystalline rocks undergoing solid-state, viscous flow by dislocation creep at comparable strain rates (Shaw 1980; Cruden 1990; Talbot 1999, and references therein). Some experimentalists have predicted that as little as 5 vol. % melt can reduce the strength of continental crust by 50% (e.g. Dell'Angelo & Tullis 1988), whereas others have argued that the crust is weakened by several orders of magnitude once a critical melt percentage (10–30 vol. %, Arzi 1978) is attained. Yet deformation induces melt segregation, and partial loss of melt can cause rocks to harden (Renner *et al.* 2000), particularly if strain rates are high ($\geq 10^{-8}$ s^{-1}). Also, strain localization does not necessarily coincide with weakening; rocks can harden during localization if the deformation involves a component of dilation (Hobbs *et al.* 1990) as, for example,

during melting or syntectonic metamorphic reactions (Brodie & Rutter 1985).

Thus, a number of vexing questions remain that we will address in this paper: Does melting always involve crustal weakening, as is conventionally thought? How do rock structure and rheology affect melt segregation, transport and emplacement on different time and length scales? What are the driving forces and rate-controlling steps during syntectonic melt segregation and transport? Do these forces and rates differ at different levels of the crust? What is the role of melt in the long-term, high-strain rheology of the continental crust?

This paper synthesizes field and experimental studies of deformed rocks and rock analogues, to characterize the structure and rheology of fault zones in partially melted continental crust. In the next section of this paper, we describe the strain- and depth-dependent mechanical transitions in the crust that govern high-strain crustal rheology. We then propose a conceptual model of melt-assisted creep punctuated by melt-induced fracturing and melt flow along dilatant shear surfaces. A fracture analysis of such melt-filled shear surfaces in anatectic rock allows us to place upper limits on its strength at the time of flow and fracturing. We then cast our model of anatectic flow in the broader context of strain-dependent changes in melt permeability. In particular, we propose two strain-dependent melt segregation thresholds that separate three modes of syntectonic melt flow, each of which is related to strain localization and dilation on a different length scale. We then apply the concepts in the previous sections to answer the questions posed above. In so doing, we refer to two exhumed fault zones that offer a rare glimpse of rheological transitions and syntectonic magmatic structures. We conclude with a model for the transient thermomechanical properties of melt-bearing fault zones and mention some of the implications of this model for the dynamics of basins, orogens and magmatic arcs.

Structure and rheology of crustal-scale fault zones containing melt

Depth-dependent changes in fault zones

The structure and rheology of fault rocks change with depth, as shown in the profile in Fig. 2a through a prototypical fault zone. Unlike most generic models, this fault zone contains melt at its base. Cataclasites in the brittle upper crust grade downward to mylonites undergoing viscous, solid-state flow (Sibson 1977, 1986; Scholz 1990), which in turn yield to partially melted gneisses and segregated melts undergoing anatectic flow at depth. This tripartite fault structure is generally valid for an anomalously high geothermal gradient along the shear zone ($\geqslant 30\,^{\circ}\mathrm{C\ km^{-1}}$), but to avoid overinterpretation we have not marked lithostatic pressure and temperature units on the vertical axis. Also, only a half-width section of the fault zone is shown in Fig. 2a, to emphasize our neglect of across-strike variations in fault-zone structure, particularly variations related to thermal disequilibrium during the juxtaposition of hot and cold crust across the fault zone (e.g. Handy 1990).

There is broad consensus that the strength of unmelted continental crust generally increases downward with increasing lithostatic pressure, P_l, in the brittle regime, but decreases with rising temperature, T, and/or decreasing strain rate, $\dot{\gamma}$ in the solid-state viscous flow regime (Sibson 1977, 1986; Brace & Kohlstedt 1980). Since its inception, however, this rather simple view has been modified to include transient mechanical behaviour related to rate-dependent frictional sliding (Scholz 1990, 1998, and references therein), depth-dependent increases in pore-fluid pressure in the brittle regime (Streit 1997), and polymineralic frictional–viscous flow in the solid-state, viscous regime (Handy *et al.* 1999b).

The shape of the strength v. depth curve in Fig. 2b reflects the modifications of Streit (1997) and Handy *et al.* (1999b), respectively, for the brittle and solid-state viscous flow regimes, but also includes two first-order structural–mechanistic transitions within the crust: (1) the transitional interval from brittle deformation to solid-state viscous flow (interval between dashed lines labelled b and v in Fig. 2 and subsequent figures); (2) the transition from solid-state viscous (mylonitic) flow to anatectic flow. Both transitions, particularly their mechanical characteristics, directly affect the transport and emplacement of melts in the crust.

The brittle-to-viscous transition

The brittle-to-viscous (b–v) transition is a depth interval characterized in nature by very localized deformation (Fig. 2a) and mutually overprinting relationships between cataclasites and mylonites (Handy 1998). Rock strength within this interval is expected initially to fluctuate as a result of the alternation of cataclasis and thermally activated creep mechanisms. At high strains, however, strain weakening within this depth interval is inferred to effect a decrease in strength to less than that of the over- and underlying crust

(Handy 1989), and the b–v transition narrows and rises to somewhat shallower levels (Fig. 2b; Schmid & Handy 1991). This strain weakening is attributed to switches from cataclasis (just above the initial b–v transition) or grain-size insensitive (dislocation) creep (just below the initial b–v transition) to grain-size sensitive creep (diffusion creep, diffusion- or reaction-accommodated granular flow) in fine-grained, polymineralic aggregates (Handy 1989). Rocks with small grain sizes and a grain-boundary fluid have lower laboratory strengths than coarser-grained rocks undergoing either cataclastic flow (Rutter & White 1979) or grain-size insensitive dislocation creep at comparable strain rates and temperatures (Schmid *et al.* 1977; Brodie & Rutter 1987).

Our model of a mobile, strain-dependent strength minimum just below the b–v transition modifies the widely held view of a stationary, strain-independent strength maximum at the b–v transition (e.g. Brace & Kohlstedt 1980; Sibson 1986; Scholz 1990). This view is based on the extrapolation of steady-state laboratory flow laws for rocks undergoing frictional sliding on smooth surfaces (Byerlee 1978) and thermally activated, grain-size insensitive (dislocation) creep (e.g. Weertman 1968). The rocks (usually quartzite and anorthosite, respectively, for the upper and lower crust) are tacitly assumed to have a strain-invariant microstructure, and to deform at a constant strain rate and geothermal gradient. Therefore, a strength maximum at the b–v transition as predicted with extrapolated laboratory flow laws probably exists in nature only at the onset of deformation (dashed lines in Fig. 2b) before progressive grain-size reduction weakens the rocks. As shown below, a strain-dependent strength minimum just below the ultimate b–v transition has important implications for the transport and emplacement of melts within the crust.

The transition to anatectic flow

The transition from solid-state viscous (mylonitic) flow to anatectic flow (Fig. 2a) obviously coincides with the onset of crustal melting, which varies from about 650 °C for hydrous granite (Johannes & Holtz 1996) to 750–970 °C for water-absent dehydration melting of micas in pelitic rocks at lithostatic pressures of 200–500 MPa (Singh & Johannes 1996, and references therein). Anatectic flow (Fig. 2a) involves the simultaneous operation of several deformation mechanisms in the presence of a melt. In naturally deformed, anatectic rocks, these mechanisms include dislocation creep (Rosenberg & Riller 2000), diffusion-assisted granular flow (Nicolas & Ildefonse 1996), melt-induced cataclasis (Paquet *et al.* 1981; Bouchez *et al.* 1992) and veining (Nicolas & Jackson 1982; Davidson *et al.* 1994). Melt-induced veining is analogous to hydrofracturing in rocks and soils (e.g. Shaw 1980; Wickham 1987) because melt viscosity is sufficiently low for the melt to behave as a pore fluid that counteracts normal stress on potential fracture surfaces such as grain boundaries (Law of Effective Stress or Terzaghi's Law). We use the term vein to refer generally to dilatant, melt-filled fractures that are concordant or discordant (in the sense of sills and dykes, respectively) to the structural anisotropy in the adjacent wall rock. Melt-induced veining is favoured by near- to supralithostatic melt

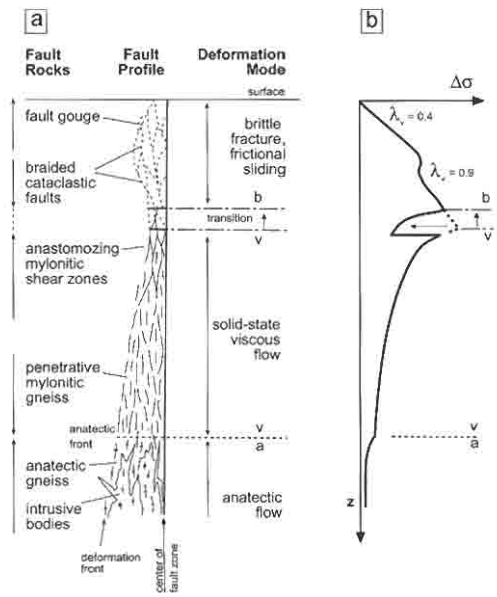

Fig. 2. Idealized section through an active, melt-bearing fault zone in continental crust at a geothermal gradient of about 30 °C km^{-1} parallel to the shear zone. (**a**) Profile showing the relative width of the fault zone from its centre to its margin (active deformation front) as a function of depth. Three deformation modes (brittle, solid-state viscous, anatectic) are separated by two major rheological transitions: the brittle-to-viscous (b–v) transition (dashed lines) and the anatectic front (dotted line) at the transition from solid-state viscous creep (marked v) to anatectic flow (marked a). (**b**) Schematic strength v. depth curve for the fault zone in (**a**). Strength curve in the brittle domain from Streit (1997) includes depth-dependent change in the pore-fluid factor, λ_v ($\lambda_v = P_{fluid}/P_{lithostatic}$) from 0.4 to 0.9, corresponding to hydrostatic and near-lithostatic pore-fluid pressures, respectively.

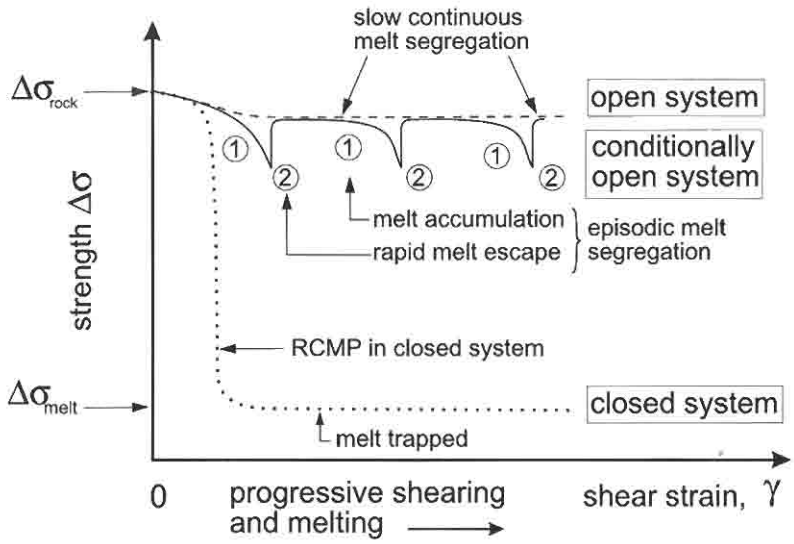

Fig. 3. Strength v. shear strain curves for three types of anatectic rock system: closed system, inspired by Arzi (1978); Van der Molen & Paterson (1979); open system, inferred from Dell'Angelo & Tullis (1988); conditionally open system, from Rosenberg & Handy (2000) and this paper. Stages numbered 1 and 2 along this curve are, respectively, periods of melt accumulation and melt escape discussed in the text.

pressures, P_m. The limit of melt-induced veining within the crust can occur on either side of the anatectic front, depending on the strain rate, melt fraction and melt pressure (see discussion below).

Deforming anatectic rocks are therefore more than just a two-phase mixture of solid and liquid; they represent an amalgam of mechanical phases with contrasting rheologies. Clearly, to characterize the bulk rheology of such a composite material with a single flow law for one, dominant deformation mechanism over the entire range of temperatures, strain rates, effective pressures, melt contents and compositions would be very unrealistic indeed. On the other hand, some structural and mechanistic simplifications are necessary to predict the bulk rheology of anatectic rocks. To model successfully the rheology of anatectic rocks is to understand the relationship between melt distribution and strain localization on the granular and supragranular scales.

Melt segregation and strain localization in closed and open systems

When attempting to understand melt segregation in a deforming rock, it is important to distinguish between melt flow in 'closed' and 'open' systems. A system is taken here to be a composite volume of deforming rock and melt. In closed (undrained) systems, melt remains within the rock on the time scale of deformation, whereas in open (drained) systems melt can flow out of, or into, the rock quickly on the same time scale. Real anatectic rocks are hybrids of these two end-member systems, but we will first consider these ideal cases before returning to nature and its complexities.

In a closed system undergoing melting, melt initially collects in the interstices of grains and forms weak pockets within a strong, load-bearing framework. Deformation takes place at constant volume and the melt pressure (P_m) is approximately equal to the mean stress in the rock. Coaxial deformation experiments at high strain rates indicate that the strength of closed systems drops drastically when the melt makes up a critical percentage or fraction of the rock (curve for closed system in Fig. 3). This so-called 'rheologically critical melt percentage' or RCMP is generally believed to coincide with the breakdown of a load-bearing framework of solid grains to a structure comprising interconnected layers of melt that accommodate almost all the strain of the partially melted rock (Renner *et al.* 2000; Rosenberg 2001). Experimentally derived values for the RCMP range from melt fractions, ϕ_m (melt volume/total volume of rock + melt) of 0.1–0.3 (Arzi 1978) to 0.4–0.6 (Lejeune & Richet 1995). At higher melt fractions and strains, the rheology of the

aggregate is dominated by that of the melt. It is important to realize that the strength drop at the RCMP occurs at a critical strain (*c.* 2% coaxial strain according to Van der Molen & Paterson (1979)) and therefore can be defined only in dynamic systems.

Unfortunately, the RCMP is often equated with a magma segregation threshold at a fixed melt fraction (Sawyer 1994; Vigneresse *et al.* 1996), above which the magma (melt + phenocrysts) is thought to become mobile and ascend from the melt source region (e.g. Wickham 1987). This is somewhat misleading, as there is strong reason to believe that the RCMP depends not only on the melt fraction, but also on the bulk strain, the bulk strain rate (Miller *et al.* 1988), and the shapes (Arzi 1978; Van der Molen & Paterson 1979) and rheologies of the constituent phases. Sawyer (1994) and Vigneresse *et al.* (1996) pointed out that melt can segregate from host rocks at melt fractions below the RCMP. In fact, the deformation experiments of Rosenberg & Handy (2001) show that syntectonic melt segregation occurs at melt fractions as small as 0.01. Both the interconnectedness of melt and the melt segregation rate increase with bulk strain as strain localizes on the granular scale (Rosenberg & Handy 2000). We therefore argue that melt segregation thresholds (henceforth abbreviated as MST) in partially melted rocks are more appropriately defined in terms of a critical shear strain for localization in the presence of melt at specified melt fraction, bulk strain rate and effective pressure (effective pressure (P_e) = lithostatic pressure (P_l) − melt pressure (P_m)).

In contrast to closed systems, open systems retain only a small amount of melt (much less than the RCMP, say $\phi_m < 0.10$) at any time during deformation, because it is assumed that the melt production rate only slightly and locally exceeds the melt segregation rate. Open systems can undergo substantial volume change through loss (or gain) of melt, and the melt pressure may deviate significantly from the mean stress in the rock. In this context, it is not important *how* the melt leaves the system but *that* it does this. Irrespective of the melt extraction mechanism(s), what is important is that most siliceous melts wet the grain boundaries of the solid grains under static (e.g. Laporte *et al.* 1997) as well as dynamic conditions (Jin *et al.* 1994; Rosenberg & Riller 2000). The melt is able to form tubules along grain boundaries and triple junctions for the rapid diffusion of melted species between grains. In this role, the melt does not accommodate the bulk strain directly, but allows diffusive mass transfer to occur on the granular scale and to accommodate the change in shape of neighbouring grains (Paterson 2001). The melt therefore enhances diffusional or granular flow of the solid grains. Deformation experiments on partially melted, hydrous granite (3–5% melt, Dell'Angelo & Tullis 1988) and melt-bearing peridotite (2–10% basalt melt, Cooper & Kohlstedt 1986; Hirth & Kohlstedt 1995a, 1995b) show that melt distributed along grain boundaries weakens aggregates undergoing dynamic recrystallization and enhances grain-size sensitive creep in very fine-grained aggregates. In the case of melt-bearing peridotite (Cooper & Kohlstedt 1986), the creep rate increased by factors of 2–5 compared with melt-free experiments that involve the same load. In partially melted granites, especially quartz-rich varieties, creep enhancement is expected to be greater because of the smaller wetting angles for quartz–granitic melt interfaces (22–23° in experiments cited by Laporte *et al.* (1997); 27° in naturally deformed granite measured by Rosenberg & Riller (2000)) compared with olivine–basaltic melt interfaces (30–40°, Cooper & Kohlstedt 1986). The strength of an open-system anatectic rock is therefore less than that of a melt-free host rock undergoing solid-state viscous creep, but significantly greater than that of a closed system or of the melt alone. This is reflected in Fig. 3, where the strength curve for the open system decreases at the onset of syntectonic melting to a constant level somewhat less than the strength of the unmelted rock.

Strain localization and episodic melt segregation in nature

Of course, no natural system is ideally open or closed on all length and time scales of deformation. The naturally and experimentally deformed rocks and rock analogues in Figs. 4 and 5 suggest that real anatectic rocks behave as conditionally open systems characterized by alternating periods of open- and closed-system behaviour.

The leucosomes in the anatectic gneisses in Fig. 4 occupy dilatant shear surfaces within the rock: the main foliation (S surfaces, Fig. 4a and b), the shear foliation (C surfaces, Fig. 4a) and a shear fracture (C′ surface, Fig. 4b). The leucosomes along the C surfaces in Fig. 4a are clearly derived from the intervening rock with the arcuate S surfaces because the C-parallel leucosomes have the same composition as the S-parallel leucosomes, the S- and C-parallel leucosomes do not truncate each other, and there are no

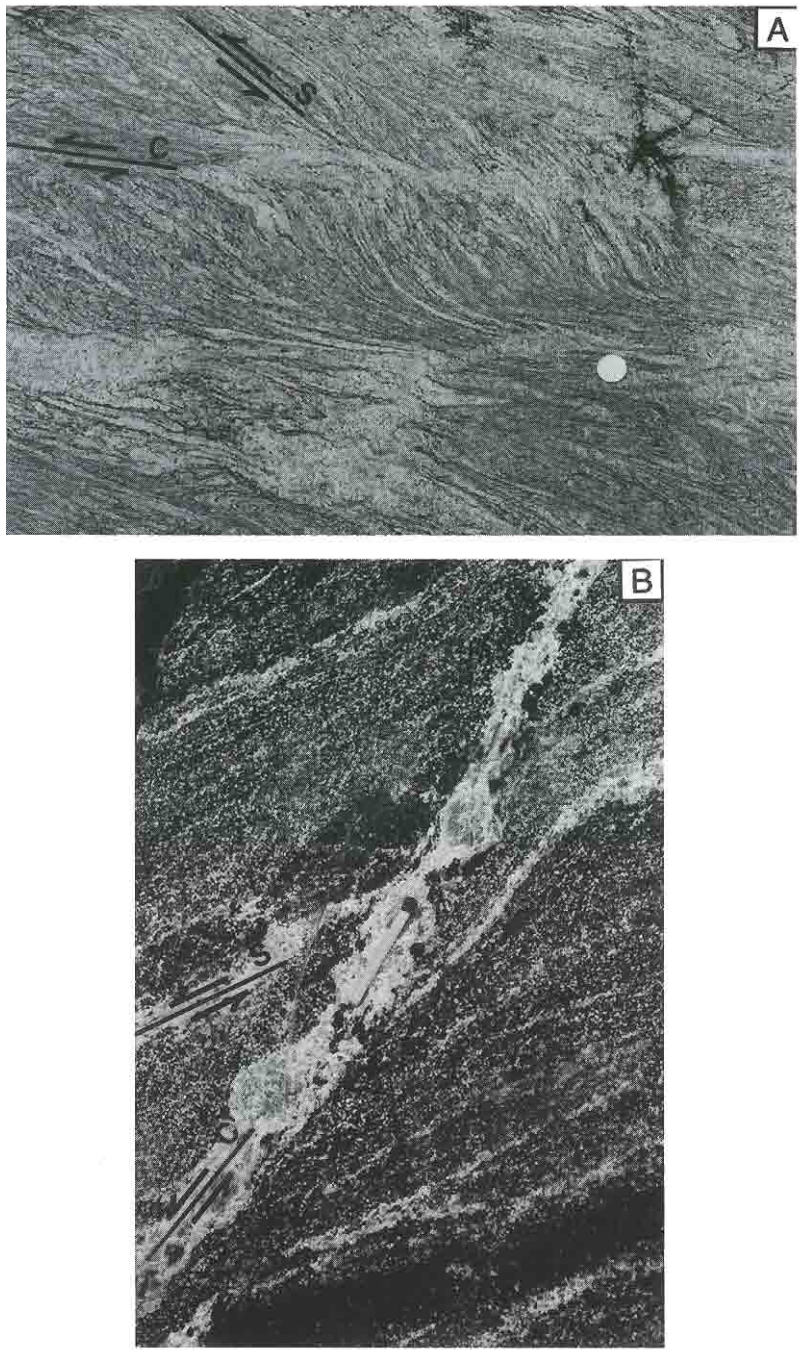

Fig. 4. Natural examples of localized deformation in the presence of melt. (**a**) Granitic leucosome occupies S and C surfaces of granitic biotite gneiss from the Southern (Insubric) Steep Belt in the Central Alps. Italian 500 Lire coin is 2.5 cm wide. (**b**) Tonalite intruded along S foliation and dilatant shear surface (C′ surface) in a garnet–pyroxene–amphibole mafic gneiss, Kapuskasing Uplift, Superior Province, Canada. Match is 4 cm long.

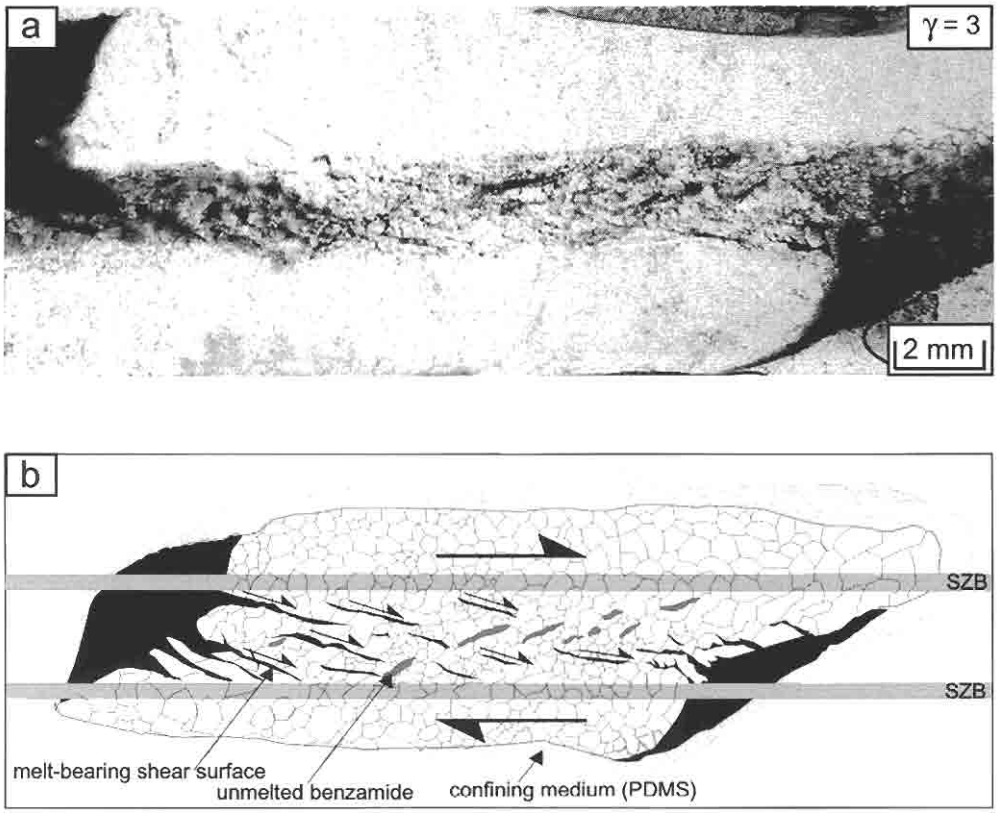

Fig. 5. Syntectonic melt segregation in a partly drained granite analogue (norcamphor–benzamide) from Rosenberg & Handy (2000). (**a**) Deformed sample viewed under plane-polarized light, perpendicular to shearing plane and parallel to shearing direction. (Note melt (back areas) and benzamide grains (grey patches) within the dynamically recrystallized norcamphor aggregate.) (**b**) Line drawing of grain aggregate in the same sample showing melt (black) along dilatant C′ shear surfaces and in sink regions at diametrically opposite ends of the shear zone. Confining medium is polydimethyl-siloxane (PDMS). SZB, shear-zone boundary.

other potential source rocks for the leucosomes in the area. The melt is therefore interpreted to have drained from source regions between the S surfaces and to have flowed into and along the dilatant C surfaces. The rock evidently remained in a partially melted state for the duration of deformation. The melt-filled C′ surface in Fig. 4b opened as an extensional shear fracture, as inferred from the displaced, angular edges of wall rock bordering the leucosome. This extensional shear geometry is diagnostic of supralithostatic melt pressure (i.e. $P_m > P_l$) and very low differential stress at the time of fracturing (Handy & Streit 1999).

Partially drained syntectonic melting experiments performed on a two-solid-phase organic aggregate (norcamphor and benzamide) directly under the optical microscope (Fig. 5) offer insight into the processes underlying melt segregation in the natural examples above. The experiments (Rosenberg & Handy 2000) were designed to simulate melt segregation during syntectonic melting of a granite and contained no more than $\phi_m = 0.1–0.15$ during the deformation. During the first increments of strain ($\gamma \leqslant 0.17$), melt that appeared along grain boundaries and interstices linked up along intergranular fractures (not shown in Fig. 5). These fractures eventually coalesced to form extensional shear surfaces within the dynamically recrystallizing grain aggregate (Fig. 5). Small amounts of melt also occupied elongate pockets in bridge structures parallel to S and linking the dilatant shear surfaces (Fig. 5). At $\gamma \geqslant 1$, the dilatant, melt-filled surfaces became conduits for the flow of melt down a local melt-pressure gradient to voids opening at diametrically opposite ends of the sample (Fig. 5). The melt fraction in the actively deforming part of the sample (between the frosted grips in Fig. 5) remained

roughly constant at about 0.1–0.15 in experiments to higher shear strains ($\gamma = 3$). This range of ϕ_m values therefore represents a dynamic equilibrium at an MST between the rates of melt production and melt segregation. In similar experiments performed on an undrained system with 0.1–0.15 water fraction (instead of melt fraction) in pure polycrystalline norcamphor (Bauer *et al.* 2000*a*), the displacement rate parallel to dilatant, fluid-filled shear surfaces fluctuated with bulk shear strain; the displacement accelerated whenever the shear surfaces coalesced, but slowed during subcritical propagation and lengthening of individual shear surfaces.

The picture that emerges from the natural and experimental observations above is one of locally episodic melt accumulation and escape (Allibone & Norris 1992; Handy & Rosenberg 1999). Natural anatectic rocks are inferred to be conditionally open systems that are characterized at the granular to outcrop scales by alternating periods of mostly closed and mostly open behaviour. The hypothetical mechanical evolution of such an anatectite is shown in Fig. 3, with the two stages labelled 1 and 2 making up one of several cycles of melt segregation.

Melting rock initially behaves as a closed system (stage 1) and weakens slightly as the melt accumulates and the solid aggregate undergoes melt-assisted creep. At a critical strain that depends on a host of variables (e.g. strain rate, melt fraction, effective pressure, wetting angle, grain size), the melt nucleates rheological instabilities (dilatant shear surfaces) that localize strain and further weaken the system. At this point, the dilatant shear surfaces serve as temporary, local sinks for melt that is squeezed and/or drawn out of the deforming source areas between the shear surfaces. As the shear surfaces lengthen and interconnect, however, they function less as melt reservoirs and more as pathways for the melt to escape. The rock has attained the MST and now behaves like an open system (stage 2). Softening as a result of strain localization on shear surfaces is now more than balanced by hardening associated with the net loss of melt to a larger melt sink in an adjacent volume of rock. The rate of melt loss, and hence also the hardening rate, is highest if the dilatant shear surfaces interconnect suddenly to form a flow network or backbone (e.g. Rutter 1997). The cycle ends when a batch of melt leaves the deforming rock.

We refer to systems with this kind of cyclical behaviour as 'conditionally open' because their openess is primarily contingent on having bulk strain rates that are sufficiently high for the melt in the creeping aggregate to build up pressure and induce hydrofracturing. We expect that higher strain rates and/or lower temperatures favour lower critical strains to the MST and hence also shorter wavelength cycles compared with those shown in Fig. 3, whereas lower strain rates and/or higher temperature would have the opposite effect. At much lower strain rates, the melt would be squeezed out of the system fast enough to pre-empt the formation of dilatant instabilities and the system would become unconditionally open in the sense described in the previous section (see Dell'Angelo & Tullis (1988) for an experimental example of this behaviour).

Upper limits on the strength of rocks undergoing anatectic flow and melt-induced veining

The rheology of conditionally open anatectic rock systems is transient and therefore impossible to characterize in terms of a steady-state flow law. Extrapolating experimental (Rutter & Neumann 1995) or theoretical (Paterson 1995, 2001; Rutter 1997) flow laws for melt-bearing aggregates undergoing dislocation creep or granular flow yields an estimate of anatectic rock strength in an open system (Fig. 3). For various reasons, however, extrapolating such flow laws is problematic (Paterson 1987) and at best yields only order-of-magnitude strength estimates.

Limits on anatectic rock strength during melt-induced veining can be obtained from the geometry of leucosomes in the partially melted rocks pictured in Fig. 4 and depicted schematically in Fig. 6a and b. End-member stress states for these rocks are shown in Mohr diagrams in Fig. 6c and d. In these diagrams, rock strength or differential stress corresponds to the diameter of the Mohr circle and is constrained in the following way. As discussed in the previous section, the structures in Fig. 4 indicate that melt-filled fractures oriented both parallel and oblique to the S foliation opened during anatectic flow. This requires the Mohr circle to touch or cross two failure envelopes for fracturing oblique and parallel to the pre-existing S foliation (respectively labelled 'tr' and '‖S' in Fig. 6) and a yield envelope for anatectic flow on this foliation (labelled 'flow on S' in Fig. 6). More specifically, the circle must be small enough to cross or touch the 'tr' envelope somewhere between this envelope's intersections with the abscissa (at $\sigma_n' = -T$) and the ordinate (at $\tau = 2T$) to account for the extensional shear geometry of

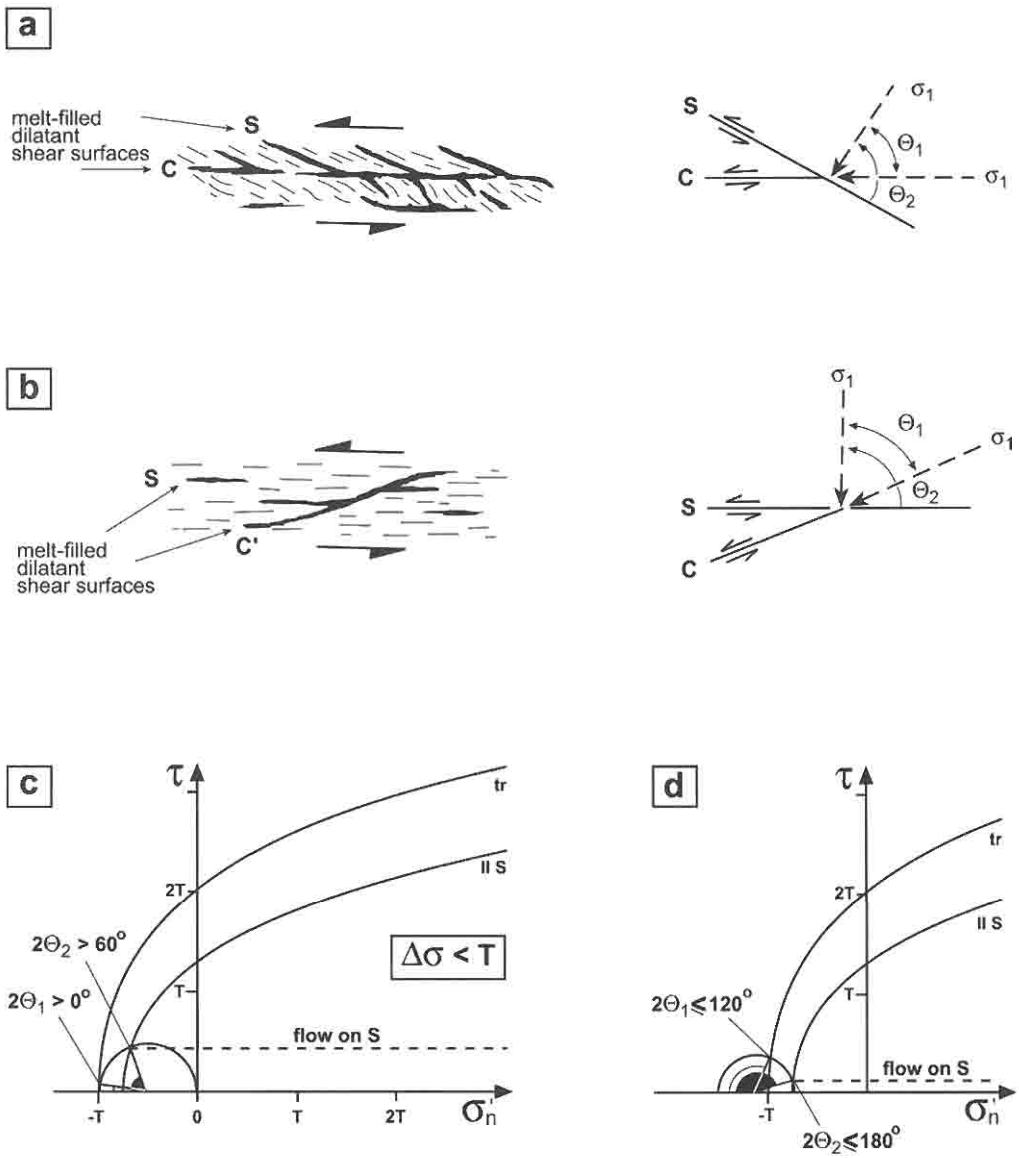

Fig. 6. Method for determining the strength limits of anatectic gneiss during coeval melt-assisted creep and melt-induced fracturing. (**a**) S and C foliations (dashes) in Fig. 4a partly filled with leucosome (black). (**b**) S and C′ surfaces in Fig. 4b filled with leucosome (black). (**c**) Mohr diagram with circle for the maximum differential stress assuming θ_1 was near 0°. θ_1 and θ_2 are fracture angles between the greatest principal stress direction, σ_1, and, respectively, the S and C′ surfaces. (**d**) Mohr diagram for unconstrained stress state (arbitrary Mohr circle) assuming θ_1 was near 60°. Horizontal and vertical axes of the Mohr diagrams are marked in units of tensile stress, T. Failure envelopes represent strength of mylonite in planes parallel to the pre-existing S foliation (‖S) and in all other directions (tr, through the rock). Horizontal envelope (dashed line) is for anatectic flow on the S foliation.

the C and C′ surfaces oblique to the pre-existing S foliation (Fig. 6). Because all melt-filled fractures accommodated a component of shear parallel to their boundaries, we also know that $\sigma_n' \leqslant 0$ and $\tau > 0$ on these surfaces.

The tr failure envelope in the Mohr diagrams of Fig. 6 was constructed by using the modified Griffith criterion for failure of flawed materials (Secor 1965). The shape and position of the parallel-S failure envelopes with respect to the tr

failure envelope reflect the lower cohesion and tensile strength of rocks parallel to pre-existing foliation surfaces, as documented in numerous experimental (Paterson 1978) and field studies (e.g. Cosgrove 1997). Melt-assisted creep is assumed to be non-dilational or nearly so, and is therefore represented by a horizontal viscoplastic yield envelope that is valid for the temperature, strain rate and average grain size in the wall rock. Both the viscoplastic yield envelope and the parallel-S failure envelope are valid only for flow and fracturing, respectively, along the pre-existing S foliation at an unfavourable angle (θ_2 in Fig. 6) to the σ_1 direction (Sibson 1985).

The measured angles between the oblique dilatant shear surfaces and the S foliation in Fig. 4a and b indicate that the fracture angles, θ_1, between the greatest principal stress axis, σ_1, and the melt-filled surfaces (C surface in Fig. 4a, C′ surface in Fig. 4b) must have been in the range of $0° < \theta_1 \leqslant 57°$ (Fig. 6a) and $0° < \theta_1 \leqslant 60°$ (Fig. 6b). In both cases, the minimum fracture angle near 0° and the presence of melt-bearing S surfaces that accommodated flow require that rock strength did not exceed the tensile strength of intact rock, T, as shown in Fig. 6c. On the other hand, the maximum possible fracture angles in both examples are near 60°, indicating that $\sigma_1' > -T > \sigma_3'$ (Fig. 6d). This information alone is insufficient to place a lower limit on rock strength at the time of veining. The Mohr circle in Fig. 6d is only one of a family of circles of variable diameter at $\theta_1 = 60°$. Unfortunately, we found no appropriate strain markers with which to reconstruct the strain ellipsoid and kinematic vorticity (Passchier & Urai 1988), and narrow the range of possible fracture angles.

The Mohr diagrams in Fig. 6 allow us to place a crude upper limit on anatectic rock strength. In a review of the rock mechanics literature, Etheridge (1983) determined that most metamorphic rocks have a tensile strength of 10 MPa or less, and in the presence of a metamorphic fluid, a value of 5 MPa is more realistic. We can therefore limit the maximum differential stress in the anatectic gneisses of Fig. 4 to somewhere in the range of 5–10 MPa. Strengths of <5 MPa are certainly conceivable; Rutter (1997, p. 106) speculated that partially melted granitic rocks have strengths of 1 MPa or less, a value apparently obtained from the undrained experiments of Van der Molen & Paterson (1979) on granite with 20% melt.

The upper limit on anatectic rock strength of 5–10 MPa is consistent with the maximum strength estimate by Handy & Streit (1999) of 10–20 MPa for anatectic, lower-crustal rocks near concordant mafic veins. Both estimates fall within the lower end of a broad range of strength estimates obtained from experimental flow laws (Kohlstedt *et al.* 1995) for quartz and feldspar aggregates undergoing dislocation creep and extrapolated to the conditions of deformation in Fig. 4. These results provide independent confirmation of the prediction that granitic crust undergoing coeval melt-assisted creep and melt-induced veining is weaker than crust undergoing solid-state viscous flow by dislocation creep.

Another interesting implication of our low strength estimates is that the tectonic overpressure (taken here to be $\sigma_m' - P_e$, the difference of the effective mean stress and effective pressure, assuming that $P_e = \sigma_3'$) is constrained to be only half of the differential stress, i.e. ⩽2–5 MPa for the range of tensile strengths above. We will return to this point below in a discussion of melt driving forces, but turn next to the mechanisms underlying syntectonic melt segregation.

Modes of syntectonic melt flow

The evolution of melt permeability with strain

Episodic melt segregation in deforming anatectic rocks can be considered in terms of a time- and strain-dependent sequence of melt segregation modes, each of which is linked to strain localization on different scales and at different strain rates, melt fractions and effective pressures. These melt segregation modes and their respective microstructures are shown schematically in a diagram of permeability v. shear strain in Fig. 7. This diagram applies to a hypothetical rock that is homogeneous on the granular scale at the onset of deformation and melting. Permeability of melt is considered subparallel to the shear-zone boundary and is therefore controlled primarily by the connectivity of melt-filled space in this plane.

The three fields on the left side of Fig. 7 correspond to distinct modes of syntectonic melt flow in open and conditionally open rocks with melt fractions less than *c.* 0.30: (1) melt percolation along wetted or partly wetted grain boundaries, commonly referred to as porous flow (e.g. Brown *et al.* 1999); (2) melt transport within discrete supragranular, dilatant shear surfaces or bands (e.g. Gapais 1989; Rey *et al.* 1992; Vauchez & Egydio da Silva 1992), referred to here as shear surface flow; (3) channel flow through a network of interconnected, dilatant shear surfaces or veins (Clemens &

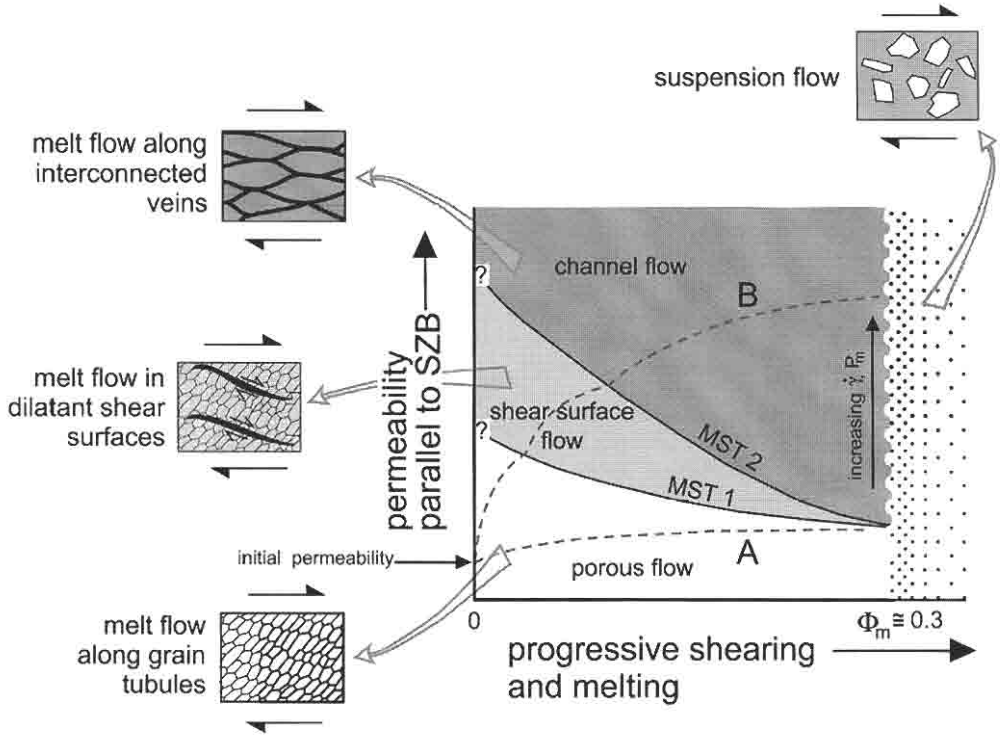

Fig. 7. Permeability of melt subparallel to the shear-zone boundary (SZB) v. shear strain for different modes of syntectonic melt flow. Insets depict microstructures corresponding to these modes, with melt-filled areas (black) set against a matrix of grains undergoing melt-assisted creep. Continuous curves represent melt segregation thresholds (MST). Dashed curves depict hypothetical evolution of permeability for progressive melting at low (A) and high (B) shear strain rates. Vertical wavy line marks transition to suspension flow (stippled field) at melt fractions, ϕ_m, of *c.* 0.3.

Mawer 1992; Rutter & Neumann 1995). The two continuous curves delimiting these fields represent MSTs that are discussed below. Two dashed curves labelled A and B show how permeability of melt evolves with structure during melting at ideal conditions of constant bulk shear strain rate. The strain rate of curve B is greater than for curve A. A fourth field on the right side of Fig. 7 for suspension flow at melt fractions greater than *c.* 0.30 pertains to closed systems in which melt-space is connected in all directions. This field is therefore not relevant to the discussion below. The shapes of the curves and fields in this diagram are speculative, as they are based partly on experimental data and partly on theoretical models of fluid flow in porous media. Nevertheless, the diagram is useful for discussing the possible mechanisms and rate dependences underlying the evolution of melt-filled space during deformation.

At low strain rates and melt fractions (curve A in Fig. 7), the entire system is expected to deform ductilely by one or more melt-assisted creep mechanisms (dislocation creep, granular flow, e.g. Dell'Angelo & Tullis 1988; Hirth & Kohlstedt 1995a, 1995b). In the absence of an externally imposed melt head (analogous to a hydraulic head), the melt flows because the deforming grains in the aggregate impart motion to the intragranular melt (Rutter 1997). Porous flow is slow compared with shear surface or channel flow because it is induced by changing pore size during deformation of the matrix grains. Melt connectivity and hence also permeability are expected to increase at a decreasing rate with shear strain as a result of the development of a steady-state microstructure, as indicated by the convex-upward shape of curve A in Fig. 7. Assuming that the grain boundaries remain wetted with melt throughout deformation, the overall increase in permeability is

not just due to related increases in melt fraction and porosity, but may also be due to the formation of steady-state foliations subparallel to the shearing plane (Lamoureux *et al.* 1999), or to limited intergranular fracturing during dynamic recrystallization (Rosenberg & Riller 2000) and/or diffusion-accommodated granular flow. Irrespective of the creep mechanism, however, the strain rate is slow enough that the melt is never pressured sufficiently for it to induce pervasive hydrofracturing on the supragranular scale. Rather, the melt is squeezed out as fast as or faster than the rate at which it is produced, as discussed by Dell'Angelo & Tullis (1988).

At higher strain rates (curve B in Fig. 7), the melt pressure is sufficiently high to induce intergranular hydrofracturing at the lower MST (MST 1) in Fig. 7. This threshold marks the transition from melt transport by porous flow within a ductilely deforming aggregate to melt transport primarily within dilatant shear surfaces, as previously discussed for Fig. 4. With further strain, the melt-induced fractures lengthen, localizing the strain while draining melt by porous flow from the intervening rock. The rock is conditionally open, as described in the previous section. Curve B is inferred to flatten with strain if the melt-filled dilatant shear surfaces attain a steady-state aspect ratio and spacing. A similar relationship between effective porosity and strain was observed in deformation experiments conducted at near-lithostatic fluid pressures (Fischer & Paterson 1992; Zhang *et al.* 1994) and has been linked to the formation of dilatant fluid-filled shear surfaces in dynamically recrystallizing norcamphor, a quartz analogue material (Bauer *et al.* 2000a). If dilatant shear surfaces contain overpressured melt, they can propagate like zippered veins (e.g. Rubin 1998), opening and closing in the direction of propagation along the mechanically weak foliation subparallel to the shear-zone boundary, as observed in the experiments of Bauer *et al.* (2000b).

With further shearing and melting, melt-space connectivity and permeability increase rapidly with strain as the rock crosses the second MST. There, the dilatant shear surfaces interconnect to form a network of veins subparallel to the shear-zone boundary. Curve B can flatten (Fig. 7) if either the veins that channel the melt or the vein network itself stops widening. This steady-state width represents a dynamic equilibrium in both the rheological and fluid-dynamic senses: it manifests a balance of softening and hardening processes (e.g. Means 1995) as well as a balance of processes creating and destroying interconnected, melt-filled space. Effective porosity during channel flow is estimated to vary within the range of 10–25 vol. % in metasediments undergoing anatexis, based on the assumption that minimum porosity is equal to the leucosome volume (Brown *et al.* 1999, and references therein).

Network or channel flow facilitates the rapid transport of melt down melt-pressure gradients (Rutter 1997; Brown *et al.* 1998). Examples of melt networks include leucosome channels in stromatic migmatites (e.g. Brown *et al.* 1999) and mafic vein arrays in anatectic gneisses (e.g. Escher *et al.* 1976; Hanmer *et al.* 1997; Handy & Streit 1999). These melt-bearing vein networks are analogous to fluid-flow backbones along anastomosing shear zones formed at or just below the b–v transition (Cox 1999, and references therein). Networks of fluid flow and melt flow have in common the persistence of transient, near-lithostatic to supra-lithostatic pore-fluid pressures (P_f in metamorphic rocks, P_m in anatectic rocks) during deformation (e.g. Etheridge *et al.* 1983; Handy & Streit 1999). High melt pressures are necessary to prevent vein networks from collapsing at the high lithostatic pressures and temperatures of the deep crust. Such high melt pressures are maintained only for short times because melt can escape much more quickly along dilatant shear surfaces and vein networks than can enter these *fast-drain channels by porous intergranular* flow. Rutter & Mecklenburgh (2001) have estimated that melt permeability in channel flow is up to 10^6 times that in porous intergranular flow. This considerable contrast in melt fluxes for porous flow and channel flow accounts for the episodicity of melt segregation in anatectic rocks which, like those described in the previous section, were conditionally open.

Clearly, curve B in Fig. 7 only approximates the evolution of melt permeability in naturally deformed anatectic rocks. The actual evolution is probably much more irregular than either of the idealized trajectories in Fig. 7. Melt-space connectivity (and therefore permeability) fluctuates locally with changes in strain rate and melt pressure so that trajectories for small volumes of rock are expected to cross MSTs more than once. The MSTs themselves would shift their position in Fig. 7 if melt viscosity (dependent on temperature and volatile content) or shear regime (coaxial v. noncoaxial) were to vary during deformation.

The dynamic nature of MSTs

The two MSTs in Fig. 7 pertain to rocks melting during deformation and are therefore meaningless at static (i.e. stress-free) conditions. In this sense, they are similar to the MSTs of Sawyer (1994), but differ fundamentally from the melting and crystallization thresholds proposed by Vigneresse *et al.* (1996). The latter melting thresholds depend exclusively on melt content (liquid percolation and melt escape, respectively, at 8 and 20–25 vol. % melt) and are defined on the basis of bond-percolation theory in materials with a static melt distribution. The same is true of their two thresholds in crystallizing systems (rigid-percolation and particle-locking thresholds at 55 and 25–28 vol. % melt), except that these are based on site-percolation theory for static crystal mushes.

Although we agree with Vigneresse *et al.* (1996) that the pre-deformational structures of melting and crystallizing systems at rest differ, we predict that deformation has two modifying effects on any statically defined segregation thresholds: (1) deformation would cause structures in melting and crystallizing systems to converge towards a similar if not identical steady-state structure; (2) it would lower the amount of melt at such thresholds to an extent dependent primarily on strain rate, melt pressure, shape, size, and rheologies of constituent phases, as argued above. The first effect pertains if the rates of melting or crystallization are comparable with each other and if both are lower than the rate at which the microstructure adjusts to changes in melt content. The ubiquity of melt-filled shear surfaces in both melting (e.g. Rey *et al.* 1992) and crystallizing (e.g. Gapais 1989; McCaffrey 1994; Smith 1997) magmatic rocks with a similar range of melt fractions suggests that these conditions indeed pertain in nature.

A conclusive assessment of MSTs in melting and crystallizing rocks must await the outcome of experiments designed to test the effects of deformation on such thresholds. If our analysis is correct, however, then the dynamic MSTs we defined above in Fig. 7 are equivalent in both melting and crystallizing systems.

Melt segregation, transport and emplacement in crustal-scale shear zones: a discussion with examples

To understand how the modes of syntectonic melt flow in Fig. 7 operate on different time and length scales, we turn to some case studies of igneous activity in crustal-scale fault zones. Together with the concepts developed in the previous sections, these examples provide answers to some of the questions posed in the introduction.

How do structure and rheology affect melt segregation and crustal differentiation?

The Ivrea crustal cross-section in the southern European Alps is a good example of structurally controlled crustal differentiation. This exhumed cross-section of continental crust contains the remnants of an Early Permian transtensional fault zone and related magmatic rocks (Fig. 8). The composite section in Fig. 8 depicts this fault zone at its inception in Early Permian time. Steep, oblique-slip faults bounding elongate, asymmetrical basins in the upper crust (Collio basin, Schönborn & Schumacher 1994; Cassinis *et al.* 1995) extended downwards to moderately inclined mylonites of the CMB (Cossato–Mergozzo–Brissago) Line in the intermediate to lower crust (Handy *et al.* 1999a). These mylonites contain syntectonic, gabbro–dioritic to granitic intrusive bodies with a broad range of calc-alkaline compositions (Pinarelli *et al.* 1988; Mulch *et al.* 1999). These intrusive rocks were consanguineous with Early Permian mafic and ultramafic melts in the lower crust (Mafic Complex in Fig. 8; Rivalenti *et al.* 1984; Sinigoi *et al.* 1994) and similarly aged granitic plutons in the upper crust (Baveno granites in Fig. 8; Boriani *et al.* 1992).

The oblique-slip fault in the upper crust bounds these granitic plutons, the shallowest of which intruded at a depth of *c.* 5 km (Köppel 1974) along the steeply dipping, pre-Permian schistosity of the wall rock (Fig. 8). These plutons have hydrothermal contact aureoles and locally discordant contacts (Balk 1924), but did not induce partial melting or mylonitization of the wall rock. The limit of melt-induced veining is extended around the perimeter of the plutons, well above the Early Permian b–v transition (Fig. 8). This transition is not exposed in the field as a result of overprinting and tectonic excision during later Early Mesozoic and Tertiary faulting. However, the heat advected by the granitic plutons along the fault is expected to have raised the b–v transition in their vicinity, as shown in Fig. 8.

The mylonitic shear zones in the lower crust, including those of the CMB Line (Fig. 8), attenuated and partly exhumed the intermediate to lower crust during Early Permian transtension

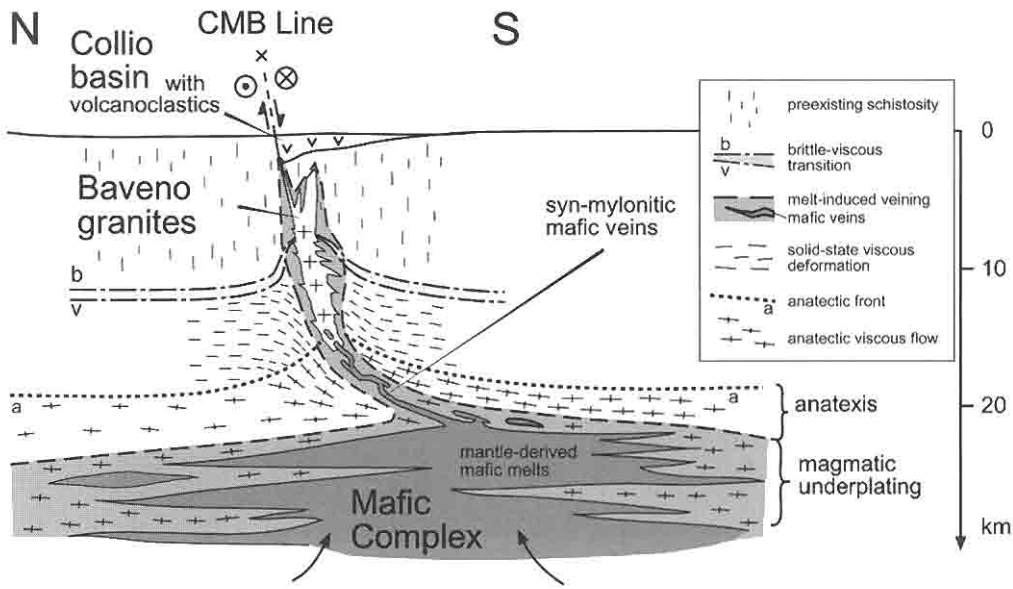

Fig. 8. Composite profile of the Ivrea crustal cross-section in Early Permian time showing the CMB Line (Cossato–Mergozzo–Brissago) and related Early Permian features. Curves for b–v transition (dashed–dotted), anatectic front (dotted) and limit of melt-induced veining (dashed) are same as in Fig. 2.

(Handy & Zingg 1991; Rutter *et al.* 1993; Quick *et al.* 1994). Mylonitization was associated with veining of mafic melts and anatexis of the metasedimentary wall rocks near these veins, both along the CMB Line (Handy & Streit 1999) and along the rim of the Mafic Complex (Snoke *et al.* 1999). The anatectic front therefore extended upwards within the crust only as far as the syntectonic mafic veins of the CMB Line, and downwards to just above the mantle-derived melts that ponded in the lower crust (Fig. 8).

The syn-mylonitic mafic veins of the CMB Line are very elongate (aspect ratios of >1000:1) and link up locally to form a vein network along the mylonitic foliation (Fig. 8). This vein geometry is obviously governed by the mechanical anisotropy of the mylonitic foliation and is consistent with low crustal strength ($\leqslant$10–20 MPa) and very high melt pressure ($\leqslant$600–700 MPa) during mafic veining (Handy & Streit 1999). The vein network channelled large amounts of mantle-derived melt from the lower to the intermediate crust, where these melts crystallized under amphibolite-facies conditions. There, anatectic melts from the mylonites near the mafic veins back-veined the latter. They fractured the partly consolidated mafic melt (angular mafic fragments in Fig. 9) and induced mingling and mixing of anatectic and mafic melts (lobate structures in Fig. 9). The products of this mixing are the aforementioned hybrid melts along the CMB Line whose broad range of main- and trace-element geochemistries spans the compositional gap between coeval gabbroic and granitic rocks, respectively, in the lower and upper crust (Mulch *et al.* 1999).

The CMB Line therefore played two important roles in differentiating the continental crust. First, it served as a melt conduit for the upward veining and channelled flow of transiently overpressured mantle-derived melts. In so doing, it advected sufficient heat to partially melt and thermally soften metasedimentary wall rocks in the lower crust. Second, it served as a melt reactor system, allowing veined mantle-derived melts to mingle and mix with anatectic melts derived from the adjacent mylonitic wall rock. The resulting hybrid melts then used the same shear zone to ascend to emplacement sites at and above the b–v transition.

The CMB fault zone functioned like a conditionally open system on the crustal scale in that it accommodated sporadic fluxes of melt into and out of the granite source region within mylonites at the base of the intermediate crust and in the lower crust. Melt veining and mixing within the active shear zone must have happened very quickly, judging from the short crystallization times predicted by thermal modelling of the hybrid veins along the CMB Line (seconds to years, Handy & Streit 1999). Thus,

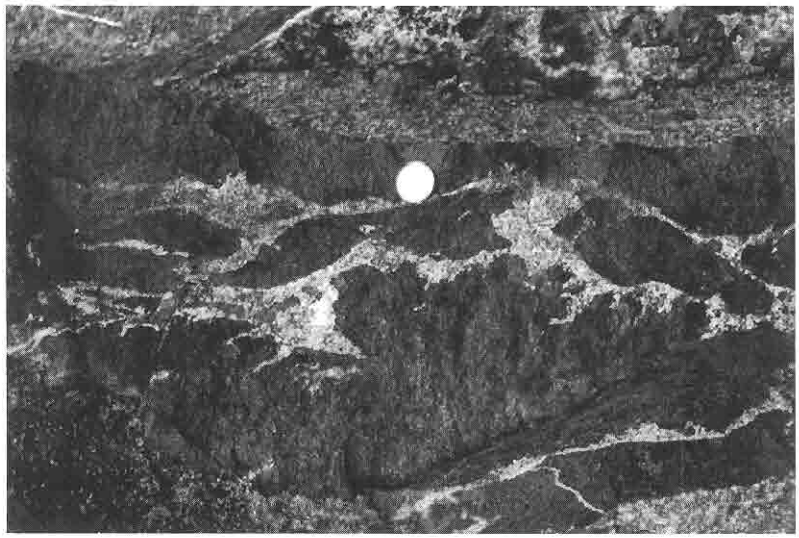

Fig. 9. Concordant hybrid vein along the CMB Line containing fragments of partly consolidated mafic melt within a matrix of felsic melt. The mafic rock comprises hornblende–plagioclase with minor amounts of retrograde biotite and has a gabbro–dioritic geochemistry. The felsic rock is granitic and is derived from anatectic melt in the mylonitized metasedimentary wall rock. (Note fractures in mafic rock filled with felsic rock (lower right side) and lobate structures at their interface (across centre) indicative of mingling and assimilation.) Italian 100 Lire coin is 2.7 cm wide.

individual magmatic pulses along the shear zone were short lived compared with the total duration of Early Permian magmatism in the Ivrea crustal cross-section (265–290 Ma, radiometric ages compiled by Handy *et al.* 1999*a*).

The case study above suggests that rapid melt segregation and transport on the crustal scale are sited along shear zones because there the rocks are sufficiently anisotropic and weak, and melt pressures high enough for the rock to cross one or both of the MSTs in Fig. 7. Porous granular flow appears to be restricted to chemically and structurally more homogeneous rocks, for example, in the asthenosphere beneath slow-spreading mid-ocean ridges (Kelemen *et al.* 1997) or possibly in parts of the Archaean lower to middle crust that underwent partial convective overturn above huge volumes of underplated mafic melt (e.g. Pilbara Craton, Collins *et al.* 1998). Otherwise, inherited lithological heterogeneities tend to localize strain and focus melt flow.

How does rheology affect melt transport and emplacement?

Insight into this question comes from the Insubric Line and Bergell pluton, which form part of the late-orogenic transpressive Periadriatic fault system sited at the retro-wedge of the Tertiary Alpine orogen (Fig. 10). The reconstructed section in Fig. 10a shows that the steep Insubric mylonites contain the concordant feeder dyke of the Bergell pluton and extend down to where they tapped mantle-derived melts ponded at the base of previously subducted continental crust (Schmid *et al.* 1996). The Periadriatic Line and associated Tertiary plutons are interpreted to have formed in response to continuing collision above a detaching lithospheric slab (Dietrich 1976; von Blanckenburg & Davies 1995).

Davidson *et al.* (1996) proposed a two-stage emplacement history for the Bergell pluton (Fig. 10b and c). In the first stage, melt transport occurred within the steep, concordant feeder vein and emplacement outside the Insubric mylonite belt into space created by the northward movement of two Penninic nappes (the Tambo and Suretta nappes; Schmid *et al.* 1990) beneath the Late Cretaceous Tethyan suture. By the time of the Mid-Tertiary Bergell intrusion, the rocks just below this suture were the site of an east-dipping normal fault (Turba normal fault in Fig. 10c; Nievergelt *et al.* 1996). This normal fault was an active b–v transition that juxtaposed cold (<250 °C), brittle Austroalpine units in its footwall against warm, mylonitic Penninic units in its exhuming footwall (350–430 °C; Ferreiro Mählmann 1996). The steep Insubric mylonites were also an

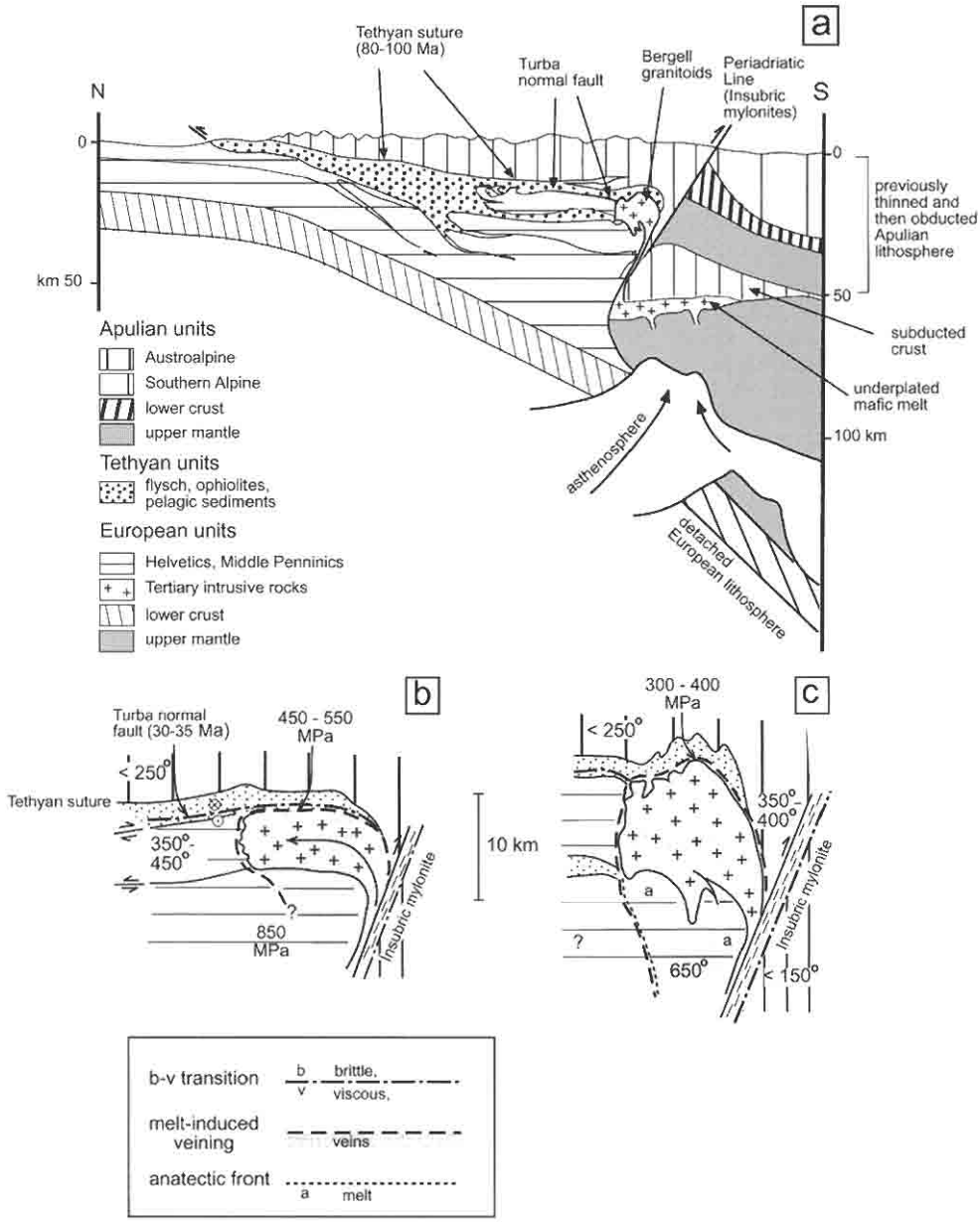

Fig. 10. (**a**) Cross-section of Tertiary Alpine Orogen (Central Alps) including the Bergell pluton and its elongate feeder vein along the Insubric Line (from Schmid *et al.* 1996, fig. 8e); (**b**) and (**c**) two-stage emplacement of Bergell pluton showing b–v transitions, anatectic front and limit of melt-induced veining (modified from Davidson *et al.* 1996, fig. 10). Pressure and temperature estimates from Davidson *et al.* (1996); Ferreiro Mählmann (1996); Trommsdorff & Connolly (1996).

active b–v transition at the time of intrusion, as they juxtaposed hot Tertiary metamorphic rocks of the Penninic basement against cold (<150 °C) pre-Alpine metamorphic rocks of the southern Alpine basement. In the second stage, continued melt transport within the feeder vein and pluton growth (ballooning) were coeval with lateral, north–south shortening (folding) and east–west stretching of the by then partly crystallized pluton. Emplacement during this

second stage involved melt-induced veining and stoping along the upper sides of the pluton, and anatectic flow and folding above, along and beneath the pluton's base (Rosenberg *et al.* 1995). Although the wall rocks along the structurally higher margins of the pluton underwent contact metamorphism (Trommsdorff & Nievergelt 1983, and references therein), the temperatures and fluid activities during intrusion of these rocks were evidently not sufficiently high to induce partial melting and anatectic flow. A dashed line in Fig. 10b and c indicating the limit of melt-induced veining is therefore drawn around the pluton margin and extended downward to include the upper amphibolite facies anatectic gneisses (Fig. 4a) beneath the pluton. This dashed line truncates the Turba mylonites in Fig. 10c, in accordance with the observation that the Turba mylonites are locally cut by the Bergell granites (Nievergelt *et al.* 1996).

The evolution above reveals several important aspects of rheological control on melt ascent. First, the Bergell pluton initially intruded mylonitic crust that was bounded by two active b–v transitions: the subhorizontal Turba normal fault above and the steep Periadriatic mylonite belt to the south (Fig. 10b). Thus, melt-induced veining occurred well above the anatectic front and affected active mylonitic rocks just below and to the north of these transitions. The mylonitic zones were weak parallel to their foliations, as described above. The Insubric mylonites channelled the melt upwards within a long, concordant feeder vein, whereas the Turba mylonites arrested its further ascent. Together with the sink created by the northward movement of the Penninic nappes, these mylonites were responsible for the fist-like geometry of the pluton. Second, for large-scale similar folds to develop at the base of the Bergell pluton during the second stage (Fig. 10c) the partly crystallized melts within the pluton must have acquired a strength comparable with that of the anatectic country rocks beneath it (Davidson *et al.* 1996). Third, melt-induced veining during the second stage extended slightly above the defunct b–v transition at the Turba mylonite zone, indicating that ancient b–v transitions do not form barriers to intrusions.

We emphasize that mylonite below a b–v transition is an effective barrier to melt propagation only if two conditions are met: (1) the mylonitic foliation must obviously be oriented at high angles to the direction of magma ascent; (2) it must be active in order for the flow stress to be sufficiently low for the pressurized melt to induce extensional shear fracturing parallel to this foliation. This notion contrasts with other explanations that invoke the viscous strength maximum at (rather than a strength minimum just below) the b–v transition as a hindrance to melt ascent (e.g. Kriens & Wernicke 1990). Once melt ponds below the b–v transition, the thermal anomaly engendered by the melt accentuates the already existing strength minimum parallel to the foliation. Alternatively, Lister & Baldwin (1993) proposed that the b–v transition along the mylonitic front or metamorphic carapace of metamorphic core complexes was induced by the steep thermal gradients in the roofs of syntectonic sills (site 7 in Fig. 1). Only if the melt pressure increases to supralithostatic values can melt fracture through an active b–v transition. This probably happens regularly for magmas to reach the surface, as in the case of the Early Permian volcanism in the southern Alps (Fig. 8).

What are the rate-controlling processes during syntectonic melt segregation and transport? Do the rates of these processes vary with crustal level?

The pattern of curves for the anatectic front and the limit of melt-induced veining in Figs 8 and 10 has interesting implications for the relative rates of veining, heating and cooling in fault zones. In both the CMB and Insubric examples, the limit of melt-induced veining was frozen above the anatectic front. Because the anatectic rocks below this front supplied melt to the propagating veins above, anatexis and veining are linked processes that presumably cease at about the same time at the end of deformation. The distribution of curves in Figs. 8 and 10 is therefore an indication that melt-induced veining was fast compared with heating and melting of the wall rocks away from the veins in the fault zone. This is consistent with model studies predicting that overpressured, melt-filled veins propagate very quickly. Because mafic melts are one to three orders of magnitude less viscous than hydrous granitic melts (Clemens & Petford 1999), they propagate at much higher velocities (metres to kilometres per second, Handy & Streit 1999) than the latter (millimetres to centimetres per second, Clemens & Petford 1999). Either of these ranges is much greater than the characteristic thermal diffusion rate in basement rocks ($0.1-1\ mm\ s^{-1}$). Estimates for time to melting and melt segregation range from months to years (Sawyer 1991) or even hundreds to thousands of years (Huppert & Sparks 1988). Thus, the limit of melt-induced veining in pro-

grade fault zones will always ascend rapidly ahead of a slower, broadening anatectic front that marks the onset of melting and anatectic flow at depth. Given the different rates of vein propagation for mafic and felsic melts, one can even distinguish limits of veining for these two melt compositions. In the case of the CMB Line, field observations indicate that the upper limit of mafic melt-induced veining corresponds to the anatectic front (Fig. 8).

As mentioned above, the rate-limiting step in conditionally open systems such as the CMB Line is likely to be anatexis and/or the porous flow of melt in the source rock to dilatant sites (shear surfaces or veins). The rate of melting depends primarily on temperature, whereas the rate of porous flow (i.e. the melt flux) is a complex function of the melt viscosity, the melt pressure gradient in the direction of flow, and the permeability of the grain aggregate. All of these factors in porous flow are themselves functions of other factors: the melt viscosity varies with temperature and volatile content (Clemens & Petford 1999), the pressure gradient depends on the dilational rate of the veins and/or on the strain rate and creep mechanism(s) in the aggregate (Rutter 1997; Paterson 2001), and the permeability is a function of the porosity and tortuosity of the aggregate (Brown *et al.* 1999). Because both melting rates and porous flow rates are strongly temperature dependent, the rate at which deforming source rocks supply melt to dilatant shear surfaces or veins increases with increasing heat flow and strain rate in the fault zone.

A striking feature of rocks from numerous ancient anatectic fault zones is that they preserve fresh magmatic and solid-state deformational microstructures, even from deep crustal levels. This suggests that temperature and stress drops at the end of deformation were sufficiently fast to prevent structures from re-equilibrating later with ambient retrograde conditions. The time to crystallization of melt in veins is short compared with the total cooling time to the temperature of the wall rock (Paterson & Tobisch 1992). Davidson *et al.* (1992) calculated that even a 1 km thick tonalite vein at 700 °C in a wall rock at a temperature of 500 °C crystallizes after only 90 ka. The degree of preservation of magmatic structures generally increases upwards within fault zones, primarily as a result of increased rates of cooling and stress decay at progressively shallower levels of the crust. Knipe (1989) estimated that differential stress must decrease at a rate of at least 1 MPa per 10^3–10^4 a to preserve dislocation creep microstructures in quartz formed at temperatures of 300–400 °C and 50 MPa differential stress. Higher temperatures require faster stress drops to preserve these solid-state microstructures. This range of stress decay rates (10^{-3}–10^{-4} MPa a^{-1}) is therefore a lower limit on the stress decay rates necessary to prevent magmatic microstructures formed at much higher temperatures from equilibrating with stress under subsolidus conditions.

The constraints above indicate that although there are order of magnitude differences in the rates of processes active during melt segregation and transport, none of these processes are slow. They operate on time scales that are remarkably short (10^3–10^5 a) compared with the duration of orogenesis or rifting (10^6–10^7 a).

What are the driving forces of melt ascent and emplacement?

The preservation of magmatic structures within vein networks along the CMB Line (Fig. 8) and within the long, narrow Bergell feeder vein along the Insubric Line (Fig. 10a) indicates that veins remained melt filled along their length on the same time scale as required for the melt to cool below the solidus. The vein geometry further suggests that the melts were overpressured, thus preventing the veins from collapsing (Berger *et al.* 1996; Handy & Streit 1999).

Several driving forces that have been proposed for syntectonic melt ascent within the crust, such as tectonic overpressure (Hutton 1998; De Saint Blaquat *et al.* 1998) or local dilation and compression along uneven fault planes (D'Lemos *et al.* 1992), cannot explain the melt distribution in our examples for the following reasons: (1) tectonic overpressure is a viable driving force for ascending melts only in compressional or transpressional settings (e.g. magmatic arcs, De Saint Blaquat *et al.* 1998), not in transtensional faults such as the CMB Line; (2) no irregular, dilating fault surfaces were seen on a large scale that could have squeezed or sucked the melt up or down the CMB or Insubric fault zones; (3) the low strengths estimated for the veined anatectic rocks from the CMB Line and the examples in Fig. 4 suggest that tectonic overpressure in partially melted intermediate to lower crust does not exceed 2–5 MPa (recall discussion above). These values are two orders of magnitude less than values cited elsewhere for tectonic overpressure (e.g. 500 MPa, Bott & Kuznir 1984, in De Saint Blaquat *et al.* 1998) and are also significantly lower than stresses at depth associated with the density contrast between melt and

wall rock (Hogan *et al.* 1998). Rutter & Mecklenburgh (2001) have postulated that tectonically induced differential stress gradients (*c.* 1 MPa m^{-1}) exceed the gravitationally induced gradient (*c.* 0.003 MPa m^{-1}) only over relatively small distances (millimetres to metres) between fast-drainage conduits (veins, dilatant shear surfaces). Therefore, deformation cannot squeeze melt over greater distances, where gravity acting on density contrasts between melt and wall rock must be the dominant force driving vein propagation and melt ascent.

The dominance of gravity as the dominant driving force explains why the direction of melt flow within many fault zones, including the CMB and Insubric Lines, is independent of the orientation of the strain ellipsoid as inferred from mineral stretching lineations and leucosome rods in anatectic and mylonitic wall rocks. Although melt flow parallel to the main stretching axis is certainly possible (as documented in the study by Brown & Solar (1998) of melt flow along prolate-strain structures), it is not the rule in most shear zones.

The aspect ratio of mafic veins along the CMB Line is much less than that of the kilometre-long, millimetre-wide dykes predicted theoretically by Rubin (1998) with fracture and fluid mechanics. We suspect that the unrealistic vein dimensions obtained in the models of Rubin (1998) partly reflect the assumption that channelled melt flow in veins is perfectly laminar. They may also indicate that the flow of melt from its source in a dynamically recrystallizing aggregate into the vein is more efficient than assumed in his models. Neverthess, the basic conclusion of Rubin (1998) that veins (his dykes) can drain large amounts of melt into compliant plutons is consistent with our own conclusions for plutons beneath the b–v transition.

What is the long-term, high-strain rheology of the continental crust? Does melting always involve crustal weakening?

Crustal rheology during a complete magmatic cycle can be understood in terms of three stages of fault zone development, shown in Fig. 11: (1) a juvenile stage, with incipient melting at depth; (2) a climax stage, at the peak of magmatic activity; (3) a mature stage, just after the cessation of magmatism. Each of these stages has a characteristic distribution of melt, fault rocks and rheological transitions, depicted in the left-hand column of Fig. 11. The middle and right-hand columns show the corresponding transient geotherms and strength profiles. The temperature and strength curves in Fig. 11 were drawn by hand rather than calculated, to avoid pitfalls associated with thermal modelling of complex structures or with extrapolating laboratory flow laws to natural conditions. Nevertheless, they reflect the basic laws of thermal conduction and advection as applied to fault rocks with frictional and viscous rheologies. Fiducial temperature values at the b–v transition and anatectic front have been discussed above for Fig. 2.

Incipient heating during the juvenile stage (Fig. 11a) clearly weakens the base of fault zones. The primary cause of weakening is the enhancement of thermally activated dislocation creep (glide-plus-climb) in quartz and feldspar of the wall rocks. We note that incipient melting of wall rocks does not necessarily lead to weakening of the residue; partial melting can lower the water fugacity in unmelted rock and therefore inhibit hydrolytic weakening (Karato 1986). However, local hardening associated with this effect is probably masked once the melt is sufficiently abundant to induce diffusion-accommodated granular flow and thus weaken the rock.

Although mafic melts have low viscosities ($\log \eta$ of 1–3 Pa s according to Clemens & Petford (1999)), veins containing mafic melt are not expected to accommodate much bulk strain and affect the fault rheology significantly unless they form networks that remain open on time scales approaching that of a magmatic cycle (10^3–10^5 a; see below). The example of the CMB Line indicates that mafic veins propagate sporadically and crystallize very quickly (seconds to months, Handy & Streit 1999). Therefore, even if they form networks, mafic veins will actually harden rather than weaken the fault zone in the long term.

Increased strain rate as a result of weakening at the base of fault zones is expected to load the upper crust to an extent dependent on the mechanical coupling at the b–v transition. A high degree of coupling, favoured by low strains, and uniform crustal composition and structure, will obviously load the intermediate and upper crust rapidly. The corresponding increase in strain rates at these crustal levels can be expected to depress the b–v transition within the crust. Mechanical coupling is reduced, however, where inherited structural or compositional heterogeneities nucleate instabilities that localize strain.

During the climax stage (Fig. 11b), massive heat advection as a result of the intrusion of hot

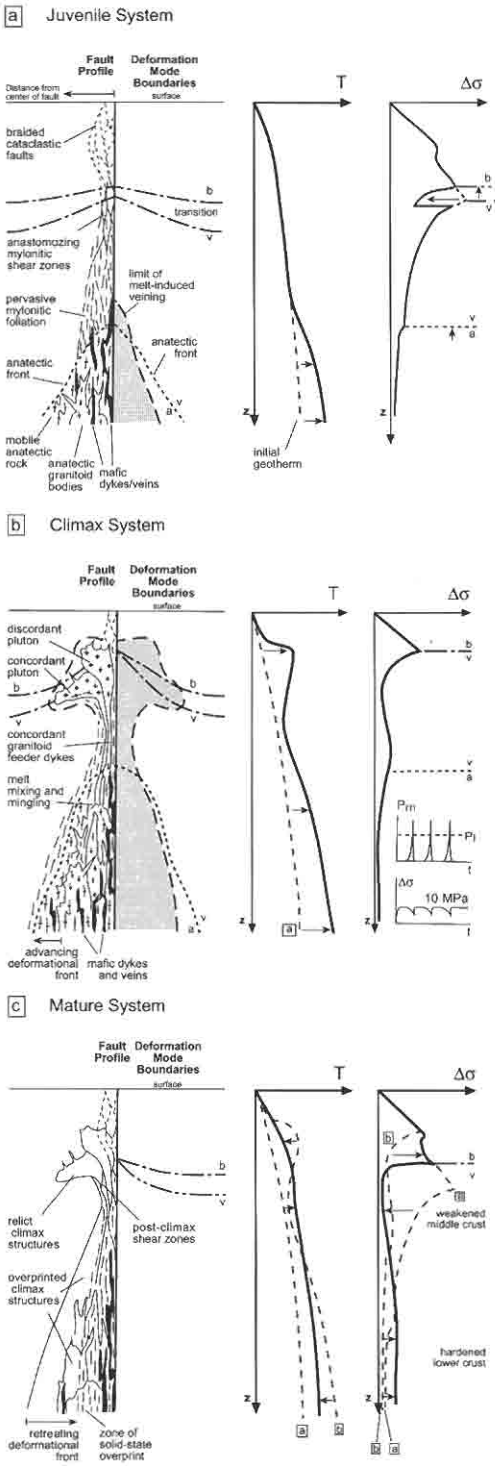

basic melts at the base of the fault zone drives the anatectic front to shallower depths and weakens all levels of the fault zone substantially. Strengths of 5–10 MPa derived in this paper (Fig. 6) represent an upper limit on the average strength of rocks undergoing anatectic flow at intermediate to deep levels of the fault zone at this stage. Higher in the intermediate crust, granitic feeder veins that connect plutons with the anatectic melt-source rocks at depth (Fig. 11b) can accommodate large displacements if they are sufficiently thick and the melt pressure remains high enough for them to remain open for a substantial time. The Bergell feeder vein in Fig. 10 or the kilometre-thick Valdez Creek tonalite within the MacLaren Glacier metamorphic belt in Alaska (Davidson *et al.* 1992) are good examples of such syntectonic veins. Davidson *et al.* (1992) estimated that the Valdez Creek tonalite accommodated a displacement of at least 10 km within the 90 ka to crystallization.

As shown in the examples of the Insubric and CMB Lines, the strength minimum just below the b–v transition is also driven upward and hinders ascent of granitic melts into the upper crust. The ponding of granitic melts just below this rheological transition engenders a local thermal bulge, which further reduces rock strength and accentuates the role of this level as an important intracrustal detachment horizon. Detachment will also occur at any depth interval where anatectic rocks are capped by stronger, less permeable rock layers (not shown in Fig. 11). There, anatectic rocks behave like closed systems and weaken drastically upon reaching an RCMP (recall Fig. 3).

Mature fault zones (Fig. 11c) generally harden as melts within them crystallize and the geotherm subsides. Not all parts of the fault

Fig. 11. Synthetic sections through a fault zone undergoing one cycle of syntectonic magmatism: (**a**) juvenile stage; (**b**) climax stage; (**c**) mature stage. Symbols in left column: dashed–dotted curve, brittle-to-viscous (b–v) transition; dotted curve, anatectic front at the transition from solid-state viscous creep (marked v) to anatectic flow (marked a); dashed curve, limit of melt-induced veining (stippled pattern). Other symbols in middle and right columns: bold continuous curves, temperature profiles (T v. z) and strength profiles ($\Delta\sigma$?v. z); bold dashed curves, temperature and strength profiles during previous stages labelled with boxed a and b; arrows indicate movement of curves since the previous stage(s). Inset diagrams in (**b**) show small, episodic variations in melt pressure, P_m, and strength, $\Delta\sigma$, as a function of time, t, and strain in the lower continental crust.

zone necessarily harden immediately or at the same time, however. Downward movement of the decaying thermal bulge around plutons emplaced just below the b–v transition can sustain or even accentuate weakening at intermediate levels of the fault zone whereas the over- and underlying levels cool and harden (Fig. 11c).

Fault zones or parts thereof can eventually attain strengths greater than their pre-melting strength if the melts that crystallize comprise minerals with higher solid-state creep strengths than those of the adjacent wall rock. For example, some of the crystallized mafic veins along the CMB Line (Fig. 8) are boudinaged (Handy & Streit 1999, fig. 2) and therefore represented a second, harder phase within the quartzo-feldpathic gneiss during mylonitization. The composite strength of this aggregate was greater than that of the gneiss alone, although in this case the gneisses still dominated the bulk rheology because of their interconnectedness parallel to the shear-zone boundary (Handy 1994). The large volumes of Carboniferous and Permian mafic and ultramafic intrusive rocks in the Mafic Complex (Fig. 8) probably hardened the lower crust, as indicated by the fact that most solid-state deformation during subsequent Early Mesozoic rifting was accommodated in hydrous, quartz-rich amphibolite-facies metasediments at the base of the intermediate crust rather than the crystallized intrusive rocks of the lower-crustal Mafic Complex (Handy & Zingg 1991). This observation is inconsistent with the widely held assumption that the lower continental crust is weak (e.g. McKenzie *et al.* 2000) and corroborates studies indicating that the lower continental crust beneath orogens (e.g. the Central Alps, Schmid *et al.* 1996) and non-volcanic rifted margins (Handy 1989; 1990) was as strong as or stronger than the intermediate crust and subcontinental upper mantle (Maggi *et al.* 2000).

The considerations above suggest that syntectonic melting induces cyclical weakening then hardening of the continental crust. Individual cycles coincide with melt ascent along many dilatant shear surfaces or vein networks through the crust. These episodes are relatively short lived (10^3–10^5 a) compared with the total duration of shearing at plate boundaries, which can last for as long as 10^6–10^7 a. Consequently, hardening of the crust or parts thereof may be the most important long-term mechanical effect of syntectonic melting.

Summary and conclusions

Continental fault zones in partially melted continental crust assume three roles: (1) they are agents of weakening and hardening at different levels of the crust; (2) they are conduits for the rapid movement of veined melts from melt-source regions at or below the anatectic front to melt sinks higher in the crust; (3) they serve as melt reactors in the intermediate to lower crust where mantle- and crustal-derived melts mix, mingle and fractionate to form hybrid melts. In the last capacity, they facilitate differentiation of the continental crust.

These varied roles played by fault zones are closely tied to two strain-dependent rheological discontinuities whose evolution is related to the large-scale distribution of melt: (1) a strength minimum parallel to subhorizontal mylonitic foliation in a depth interval just below the b–v transition hinders (but does not always prevent) the ascent of melts into the upper crust. Melt intrudes preferentially within this depth interval and, by advecting heat, accentuates the already existing strength minimum just below the b–v transition. However, ancient fossil b–v transitions in exhumed crust are not associated with strength minima and therefore do not hinder the ascent of melt. (2) A decrease in strength coincides with the upper depth limit of partial melting (the anatectic front). At this front, melt pressures are equal to and locally even exceed the lithostatic pressure.

The rheology of anatectic rock containing pressurized melt is determined by both the scale of strain localization and the pore connectivity, to an extent dependent on strain, strain rate and melt fraction in the rock. Below a critical shear strain, strain is homogeneous and melt is squeezed from the rock during melt-assisted dislocation creep or melt diffusion-accommodated granular creep. Beyond a critical shear strain, however, a first MST is crossed when strain localizes along dilatant shear surfaces. These surfaces draw melt from the adjacent deforming wall rock and propagate sporadically as veins. At higher strain rates and/or melt fractions, a further MST is crossed when the melt-filled shear surfaces interconnect to form vein networks. In most naturally deformed basement rocks, therefore, anatectic flow at natural strain rates in naturally deformed rocks involves a combination of melt-assisted dislocation creep or melt diffusion-accommodated granular creep, punctuated locally by melt-induced veining. Analysis of the melt-filled fracture geometries in such rocks yields upper strength limits in the range of 5–10 MPa. Thus, this type of anatectic

crust is weaker than quartzo-feldspathic rock undergoing solid-state dislocation creep at comparable temperatures and strain rates.

Dilatant shear surfaces and interconnected veins form conduits for the rapid ascent of transiently overpressured melt from melt-source rocks below the anatectic front to sinks higher in the crust. Melt ascent along such crustal scale vein networks is short lived (10^3–10^5 a), as a result of the high flux of melt within and along the veins compared with that of melt flowing into the veins. Channelled melt flow along these networks is driven primarily by gravity acting on the contrasting densities of the melt and wall rock. The direction of melt flow is therefore not related to the orientation of the incremental strain ellipsoid in most mylonitic shear zones.

The high-strain rheology of the continental crust is predicted to be episodic: long-term creep of the crust is interrupted by ephemeral weakening events associated with the propagation and interconnection of melt-filled veins on the crustal scale. Following such events, the crust hardens to pre-intrusive levels as melts crystallize. Large volumes of crystallized mafic melt in the lower crust can even increase the strength of the crust to above pre-intrusive levels.

Episodic weakening then hardening of melt-bearing fault zones in the continental crust has broad implications for other, fault-related orogenic processes. For example, melts may be at least partly responsible for triggering rapid, in some cases even repeated, exhumation of basement rock ('tectonic surges' of Hollister & Crawford 1986) along fault zones in the retro-wedges of orogens. This may apply to the central Alps, where high Oligo-Miocene exhumation rates just north of the Insubric Line have been otherwise attributed to climatically controlled drainage and erosion (Schlunegger 1999). Episodic melt-induced fault slip may also be responsible for repeated, sudden shifts in sedimentary depocentres and volcanic fields along the margins of fault-bounded basins (e.g. Tertiary Basin-and-Range: Cemen *et al.* 1985; Link *et al.* 1985; Rio Grande Rift: Olsen *et al.* 1987; Early Permian Saar–Nahe Basin, Germany: Schäfer & Korsch 1998). The notion that acute weakening of the crust is ephemeral on the time scale of faulting along plate boundaries further suggests that the dynamic problem of transmitting shear stresses across supposedly weak magmatic arcs may not be as intractable as generally believed.

The concepts presented above are largely qualitative and require quantification if they are to be tested against other causes of fault-related weakening or strengthening. This is the gauntlet thrown to numerical modellers!

This paper benefited from the insightful reviews of K. McCaffrey and E. H. Rutter, as well as the critical comments of A. Berger and M. Brown. We thank E. H. Rutter and J.-L. Vigneresse for generously sending us their manuscripts in review. Our work was supported by the German Science Foundation (DFG) in the form of grants Ha 2403/2 (SPP 'Orogene Prozesse...') and RO 2177/1 (SPP 'Genese und Transport von Silikatschmelzen').

References

ALLIBONE, A.H. & NORRIS, R.J. 1992. Segregation of leucogranite microplutons during syn-anatectic deformation: an example from the Taylor Valley, Antarctica. *Journal of Metamorphic Geology*, **10**, 589–600.

ALLMENDINGER, R.W., JORDAN, T.E., KAY, S.M. & ISACKS, B.L. 1997. The evolution of the Altiplano–Puna Plateau of the Central Andes. *Annual Review of Earth and Planetary Sciences*, **25**, 139–174.

ARZI, A.A. 1978. Critical phenomena in the rheology of partially melted rocks. *Tectonophysics*, **44**, 173–184.

BAILEY, D.K. 1992. Episodic alkaline igneous activity across Africa: implications for the causes of continental break-up. *In*: STOREY, B.C., ALABASTER, T. & PANKHURST, R.J. (eds) *Magmatism and the Causes of Continental Break-up*. Geological Society, London, Special Publications, **68**, 91–98.

BALK, R. 1924. Zur Tektonik der Granitmassiv von Baveno und Orta in Oberitalien. *Geologische Rundschau*, **15**, 110–122.

BARKER, F., FARMER, G.L., AYUSO, R.A., PLAFKER, G. & LULL, J.S. 1992. The 50 Ma granodiorite of the Eastern Gulf of Alaska: melting in an accretionary prism in the forearc. *Journal of Geophysical Research*, B5, **97**, 6757–6778.

BAUER, P., PALM, S. & HANDY, M.R. 2000*a*. Strain localization and fluid pathways in mylonite: inferences from in-situ deformation of a water-bearing quartz analogue (norcamphor). *Tectonophysics*, **320**, 141–165.

BAUER, P., ROSENBERG, C. & HANDY, M.R. 2000*b*. Deformation experiments on rock-analogue materials at controlled confining pressure: a new approach for studying strain localization at the brittle to viscous transition. *Journal of Structural Geology*, **22**, 281–289.

BERGER, A., ROSENBERG, C. & SCHMID, S.M. 1996. Ascent, emplacement and exhumation of the Bergell Pluton within the Southern Steep Belt of the Central Alps. *Schweizerische Mineralogische und Petrographische Mitteilungen*, **76**, 357–382.

BORIANI, A., CAIRONI, V., GIOBBI ORIGONI, E. & VANNUCCI, R. 1992. The Permian intrusive

rocks of Serie dei Laghi (Western Southern Alps). *Acta Vulcanologica*, **2**, 73–86.

BOTT, M.P. & KUZNIR, N.J. 1984. Origin of tectonic stress in the lithosphere. *Tectonophysics*, **105**, 1–14.

BOUCHEZ, J.L., DELAS, C., GLEIZES, G. & NÉDÉLEC, A., CUNEY, M. 1992. Submagmatic fractures in granites. *Geology*, **20**, 35–38.

BRACE, W.F. & KOHLSTEDT, D.L. 1980. Limits on lithospheric stress imposed by laboratory experiments. *Journal of Geophysical Research*, B11, **85**, 6248–6252.

BRODIE, K.H. & RUTTER, E.H. 1985. On the relationship between deformation and metamorphism with special reference to the behavior of basic rocks. *In*: THOMPSON, A.B. & RUBIE, D. (eds) *Kinematics, Textures and Deformation: Advances in Physical Geochemistry*. Springer, Berlin, 138–179.

BRODIE, K.H. & RUTTER, E.H. 1987. The role of transiently fine grained reaction products in syntectonic metamorphism. *Canadian Journal of Earth Sciences*, **24**, 556–564.

BROWN, M. 1994. The generation, segregation, ascent and emplacement of granite magma: the migmatite to crustally-derived granite connection in thickened orogens. *Earth-Science Reviews*, **36**, 83–130.

BROWN, M. & SOLAR, G.S. 1998. Shear zones and melts: positive feedback in orogenic belts. *Journal of Structural Geology*, **20**, 211–227.

BROWN, M. & SOLAR, G.S. 1999. The mechanism of ascent and emplacement of granite magma during transpression: a syntectonic granite paradigm. *Tectonophysics*, **312**, 1–34.

BROWN, M.A., BROWN, M., CARLSON, W.D. & DENISON, C. 1999. Topology of syntectonic melt-flow networks in the deep crust: inferences from three-dimensional images of leucosome geometry in migmatites. *American Mineralogist*, 11–12, **84**, 1793–1818.

BROWN, S., CAPRIHAN, A. & HARDY, R. 1998. Experimental observation of fluid flow channels in a single fracture. *Journal of Geophysical Research*, B3, **103**, 5125–5132.

BURG, J.P., BRUNEL, M., GAPAIS, D., CHEN, G.M. & LIU, G.H. 1984. Deformation of leucogranites of the crystalline Main Central Thrust Sheet in southern Tibet (China). *Journal of Structural Geology*, 5, **6**, 535–542.

BYERLEE, J. 1978. Friction of rocks. *Pure and Applied Geophysics*, **116**, 615–626.

CASSINIS, G., TOUTIN-MORIN, N. & VIRGILI, C. 1995. A general outline of the Permian continental basins in southwestern Europe. *In*: SCHOLLE, P.A., PERYT, T.M. & ULMER-SCHOLLE, D.S. (eds) *Sedimentary Basins and Economic Resources*. Springer, Berlin, 137–157.

CEMEN, I., WRIGHT, L.A., DRAKE, R.E. & JOHNSON, F.C. 1985. Cenozoic sedimentation and sequence of deformational events at the southeastern end of the Furnace Creek strike-slip zone, Death Valley region, California. *In*: BIDDLE, K.T. & CHRISTIE-BIDDLE, N. (eds) *Strike-Slip Deformation, Basin Formation, and Sedimentation*. Society of Economic Paleontologists and Mineralogists, Special Publications, **37**, 127–142.

CLEMENS, J.D. & MAWER, C.K. 1992. Granitic magma transport by fracture propagation. *Tectonophysics*, **204**, 339–360.

CLEMENS, J.D. & PETFORD, N. 1999. Granite melt viscosity and silicic magma dynamics in contrasting tectonic settings. *Journal of the Geological Society, London*, 6, **156**, 1057–1060.

COLLINS, W.J. & SAWYER, E.W. 1996. Pervasive granitoid magma transfer through the lower–middle crust during non-coaxial compressional deformation. *Journal of Metamorphic Geology*, **14**, 565–579.

COLLINS, W.J., VAN KRANKENDONK, M.J. & TEYSSIER, C. 1998. Partial convective overturn of Archean crust in the east Pilbara Craton, Western Australia: driving mechanisms and tectonic implications. *Journal of Structural Geology*, 9–10, **20**, 1405–1424.

COOPER, R.F. & KOHLSTEDT, D.L. 1986. Rheology and structure of olivine-basalt partial melts. *Journal of Geophysical Research*, B9, **91**, 9315–9323.

COSGROVE, J. 1997. The influence of mechanical anisotropy on the behaviour of the lower crust. *Tectonophysics*, **280**, 1–2, 1–14.

COX, S.F. 1999. Deformational controls on the dynamics of fluid flow in mesothermal gold systems. *In*: MCCAFFREY, K.J.W., LONERGAN, L. & WILKINSON, J.J. (eds) *Fractures, Flow and Mineralization*. Geological Society, London, Special Publications, **155**, 123–140.

CRITTENDEN, M.D., CONEY, P.J. & DAVIS, G.H. (eds) 1980. *Cordilleran Metamorphic Core Complexes*. Geological Society of America, Memoirs, **153**.

CRUDEN, A.C. 1990. Flow and fabric development during the diapiric rise of magma. *Journal of Geology*, **98**, 681–698.

DANIEL, J.M. & JOLIVET, L. 1995. Detachment faults and pluton emplacement: Elba Island (Tyrrhenian Sea). *Bulletin de la Societé Géologique de France*, **4**, 341–354.

DAVIDSON, C., HOLLISTER, L.S. & SCHMID, A.M. 1992. Role of melt in the formation of a deep crustal compressive shear zone: the McLaren Glacier metamorphic belt, South Central Alaska. *Tectonics*, **11**, 2, 348–359.

DAVIDSON, C., ROSENBERG, C. & SCHMID, S.M. 1996. Synmagmatic folding of the base of the Bergell pluton, Central Alps. *Tectonophysics*, **265**, 213–238.

DAVIDSON, C., SCHMID, S.M. & HOLLISTER, L.S. 1994. Role of melt during deformation in the deep crust. *Terra Nova*, **6**, 133–142.

DELL'ANGELO, L.N. & TULLIS, J. 1988. Experimental deformation of partially melted granitic aggregates. *Journal of Metamorphic Geology*, **6**, 495–515.

DE SAINT BLAQUAT, M., TIKOFF, B., TEYSSIER, C. & VIGNERESSE, J.L. 1998. Transpressional kin-

ematics and magmatic arcs. *In*: HOLDSWORTH, R.E., STRACHAN, R.A. & DEWEY, J.F. (eds) *Continental Transpressional and Transtensional Tectonics*. Geological Society, London, Special Publications, **135**, 327–340.

DIETRICH, V.J. 1976. Plattentektonik in den Ostalpen. Eine Arbeitshypothese. *Geotektonische Forschung*, **50**, 1–84.

D'LEMOS, R.S., BROWN, M. & STRACHAN, R.A. 1992. Granite magma generation, ascent and emplacement within a transpressional orogen. *Journal of the Geological Society, London*, **149**, 487–490.

ENGLAND, P. & MOLNAR, P. 1993. Cause and effect among thrust and normal faulting, anatectic melting and exhumation in the Himalaya. *In*: TRELOAR, P.J. & SEARLE, P. (eds) *Himalayan Tectonics*. Geological Society, London, Special Publications, **74**, 401–411.

ESCHER, A., JACK, S. & WATTERSON, J. 1976. Tectonics of the North Atlantic Proterozoic dyke swarm. *Philosophical Transactions of the Royal Society, London, Series A*, **280**, 529–539.

ETHERIDGE, M.A. 1983. Differential stress magnitudes during regional deformation and metamorphism: upper bound imposed by tensile fracturing. *Geology*, **11**, 232–234.

ETHERIDGE, M.A., WALL, V.T. & VERNON, R.H. 1983. The role of the fluid phase during regional metamorphism and deformation. *Journal of Metamorphic Geology*, 3, **1**, 205–226.

FERREIRO MÄHLMANN, R. 1996. The pattern of diagenesis and metamorphism by vitrinite reflectance and illite 'crystallinity' in Mittelbünden and in the Oberhalbstein Part 2: Correlation of coal petrographical and of mineralogical parameters. *Schweizerische Mineralogische und Petrographische Mitteilungen*, **76**, 23–46.

FISCHER, G.J. & PATERSON, M.S. 1992. Measurements of permeability and storage capacity in rocks during deformation at high temperature and pressure. *In*: EVANS, B. & WONG, T.-F. (eds) *Fault Mechanics and Transport Properties of Rocks*. Academic Press, San Diego CA, 213–252.

GAPAIS, D. 1989. Shear structures within deformed granites: mechanical and thermal indicators. *Geology*, **17**, 144–147.

HANDY, M.R. 1989. Deformation regimes and the rheological evolution of fault zones in the lithosphere: the effects of pressure, temperature, grain size, and time. *Tectonophysics*, **163**, 119–152.

HANDY, M.R. 1990. The exhumation of cross sections of the continental crust: structure, kinematics and rheology. *In*: SALISBURY, M.H. & FOUNTAIN, D.M. (eds) *Exposed Cross-Sections of the Continental Crust*. NATO-ASI Series C, **317**, 485–507.

HANDY, M.R. 1994. Flow laws for rocks containing two nonlinear viscous phases: a phenomenological approach. *Journal of Structural Geology*, 3, **16**, 287–301.

HANDY, M.R. 1998. Fault rocks from an exhumed intracrustal extensional detachment: the Pogallo ductile fault zone. *In*: SNOKE, A.W., TULLIS, J. & TODD, V.R. (eds) *Fault-related Rocks: a Photographic Atlas*. Princeton University Press, Princeton, NJ.

HANDY, M.R. & ROSENBERG, C.L. 1999. The role of large shear zones in generating and transporting melts, and in changing the rheology of Variscan continental crust. *Terra Nostra*, **99**, 93–94.

HANDY, M.R. & STREIT, J.E. 1999. Mechanisms and mechanics of magmatic underplating: inferences from syntectonic mafic veins in deep crustal mylonite. *Earth and Planetary Science Letters*, **165**, 271–286.

HANDY, M.R. & ZINGG, A. 1991. The tectonic and rheological evolution of an attenuated cross section of the continental crust: Ivrea crustal section, southern Alps, northwestern Italy and southern Switzerland. *Geological Society of America Bulletin*, **103**, 236–253.

HANDY, M.R., FRANZ, L., HELLER, F., JANOTT, B. & ZURBRIGGEN, R. 1999*a*. Multistage accretion, orogenesis and exhumation of continental crust (southern Alps, Italy and Switzerland). *Tectonics*, **16**, 1154–1177.

HANDY, M.R., WISSING, S. & STREIT, J.E. 1999*b*. Strength and structure of mylonite with combined frictional–viscous rheology and varied bimineralic composition. *Tectonophysics*, 1–4, **303**, 175–192.

HANMER, S., MENGEL, F., CONNELLY, J. & VAN GOOL, J. 1997. Significance of crustal scale shear zones and synkinematic mafic dykes in the Nagssugtoqidian orogen, SW Greenland: a re-examination. *Journal of Structural Geology*, **19**, 59–75.

HIRTH, G. & KOHLSTEDT, D.L. 1995*a*. Experimental constraints on the dynamics of the partially molten upper mantle 1: Deformation in the diffusion creep regime. *Journal of Geophysical Research*, B2, **100**, 1981–2001.

HIRTH, G. & KOHLSTEDT, D.L. 1995*b*. Experimental constraints on the dynamics of the partially molten upper mantle 2. Deformation in the dislocation creep regime. *Journal of Geophysical Research*, B8, **100**, 15441–15449.

HOBBS, B.E., MULHAUS, H.-B. & ORD, A. 1990. Instability, softening, and localization of deformation. *In*: KNIPE, R.J. & RUTTER, E.H. (eds) *Deformation Mechanisms, Rheology and Tectonics*. Geological Society, London, Special Publications, **54**, 143–166.

HOGAN, J.P., PRICE, J.D. & CHARLES GILBERT, M. 1998. Magma traps and driving pressure: consequences for pluton shape and emplacement in an extensional regime. *Journal of Structural Geology*, **20**, 1155–1168.

HOLLISTER, L.S. & CRAWFORD, L.M. 1986. Melt-enhanced deformation: a major tectonic process. *Geology*, **14**, 558–561.

HUPPERT, H.E. & SPARKS, S.J. 1988. The generation of granitic magmas by intrusion of basalt into

continental crust. *Journal of Petrology*, **29**, 599–624.

HUTTON, D.H.W. 1982. A tectonic model for the emplacement of the Main Donegal Granite, NW Ireland. *Journal of the Geological Society, London*, **139**, 615–631.

HUTTON, D.H.W. 1988*a*. Granite emplacement mechanisms and tectonic controls: inferences from deformation studies. *Transactions of the Royal Society of Edinburgh: Earth Sciences*, **79**, 245–255.

HUTTON, D.H.W. 1988*b*. Igneous emplacement in a shear zone termination: the biotite granite at Strontian, Scotland. *Geological Society of America Bulletin*, **100**, 1392–11399.

HUTTON, D.H.W. 1998. Syntectonic granites and the principle of effective stress: a general solution to the space problem? *In*: BOUCHEZ, J.L., HUTTON, D.H.W. & STEPHENS, W.E. (eds) *Granite: From Segregation of Melt to Emplacement Fabrics*. Kluwer, Dordrecht.

JIN, Z.M., BAI, Q. & KOHLSTEDT, D.L. 1994. High-temperature creep of olivine crystals from four localities. *Physics of the Earth and Planetary Interiors*, **82**, 55–64.

JOHANNES, W. & HOLTZ, F. 1996. *Petrogenesis and Experimental Petrology of Granitic Rocks*. Springer, Heidelberg.

KARATO, S. 1986. Does partial melting reduce the creep strength of the upper mantle? *Nature*, **318**, 309–310.

KELEMEN, P.B., HIRTH, G., SHIMIZU, N., SPIEGELMAN, M. & DICK, H.J.B. 1997. A review of melt migration processes in the adiabatically upwelling mantle beneath oceanic spreading ridges. *Philosophical Transactions of the Royal Society of London, Series A*, **355**, 283–318.

KNIPE, R.J. 1989. Deformation mechanisms—recognition from natural tectonites. *Journal of Stuctural Geology*, **11**, 127–146.

KOHLSTEDT, D.L., EVANS, B. & MACKWELL, S.J. 1995. Strength of the lithosphere: constraints imposed by laboratory experiments. *Journal of Geophysical Research*, B9, **100**, 17587–17602.

KÖPPEL, V. 1974. Isotopic U–Pb ages of monazites and zircons from the crust–mantle transition and adjacent units of the Ivrea and Ceneri Zones (Southern Alps, Italy). *Contributions to Mineralogy and Petrology*, **43**, 55–70.

KRIENS, B. & WERNICKE, B. 1990. Characteristics of a continental margin magmatic arc as a function of depth: the Skagit–Methow crustal section. *In*: SALISBURY, M.H. & FOUNTAIN, D.M. (eds) *Exposed Cross-Sections of the Continental Crust*. NATO-ASI Series, C, **317**, 159–174.

LACHENBRUCH, A.H., SASS, J.H. & GALANIS, S.P. 1985. Heat flow in southernmost California and the origin of the Salton Trough. *Journal of Geophysical Research*, **90**, 6709–6736.

LAMOUREUX, G., ILDEFONSE, B. & MAINPRICE, D. 1999. Modeling the seismic properties of fast-spreading ridge crustal low-velocity zones: insights from Oman Gabbro textures. *Tectonophysics*, **312**, 283–302.

LAPORTE, D., RAPAILLE, C. & PROVOST, A. 1997. Wetting angles, equilibrium melt geometry, and the permeability threshold of partially molten crustal protholiths. *In*: BOUCHEZ, J.L., HUTTON, D.H.W. & STEPHENS, W.E. (eds) *Granite: From Segregation of Melt to Emplacement Fabrics*. Kluwer, Dordrecht, 31–54.

LEJEUNE, A., RICHET, P. 1995. Rheology of crystal-bearing silicate melts: an experimental study at high viscosities. *Journal of Geophysical Research*, **100**, 4215–4229.

LINK, M.H., ROBERTS, M.T. & NEWTON, M.S. 1985. Walker Lake Basin, Nevada: an example of Later Tertiary (?) to Recent sedimentation in a basin adjacent to an active strike-slip fault. *In*: BIDDLE, K.T. & CHRISTIE-BIDDLE, N. (eds) *Strike-Slip Deformation, Basin Formation, and Sedimentation*. Society of Economic Paleontologists and Mineralogists, Special Publications, **37**, 105–126.

LISTER, G.S. & BALDWIN, S.L. 1993. Plutonism and the origin of metamorphic core complexes. *Geology*, **21**, 607–610.

MAGGI, A., JACKSON, J.A., MCKENZIE, D. & PRIESTLEY, K. 2000. Earthquake focal depths, effective elastic thickness, and the strength of the continental lithosphere. *Geology*, **28**, 495–498.

MCCAFFREY, K.J.W. 1992. Igneous emplacement in a transpressive shear zone: Ox Mountains igneous complex. *Journal of the Geological Society, London*, **149**, 221–235.

MCCAFFREY, K.J.W. 1994. Magmatic and solid state deformation partitioning in the Ox Mountains Granodiorite. *Geological Magazine*, **131**, 639–652.

MCKENZIE, D., NIMMO, F., JACKSON, J., GANS, P.B. & MILLER, E.L. 2000. Characteristics and consequences of flow in the lower crust. *Journal of Geophysical Research*, B5, **105**, 11029–11046.

MEANS, W.D. 1995. Shear zones and rock history. *Tectonophysics*, **247**, 157–160.

MILLER, C.F., WATSON, E.B. & HARRISON, T.M. 1988. Perspectives on source, segregation and transport of granitoid magmas. *Transactions of the Royal Society of Edinburgh: Earth Sciences*, **79**, 135–156.

MULCH, A., ROSENAU, M.R., DÖRR, W., HAACK, U. & HANDY, M.R. 1999. U–Pb ages of syn-mylonitic mafic and granitoid veins in the middle to lower continental crust (Ivrea–Verbano Zone, CH and I). *Terra Nova*, **99**, 150.

NELSON, K.D. & 27 OTHERS 1996. Partially molten middle crust beneath Southern Tibet: synthesis of Project INDEPTH results. *Science*, **274**, 1684–1687.

NICOLAS, A. & ILDEFONSE, B. 1996. Flow mechanism and viscosity in basaltic magma chambers. *Geophysical Research Letters*, **23**, 2013–2016.

NICOLAS, A. & JACKSON, M. 1982. High temperature dikes in peridotites: origin by hydraulic fracturing. *Journal of Petrology*, **23**, 568–582.

NIEVERGELT, P., LINIGER, M., FROITZHEIM, N. & FERREIRO MÄHLMANN, R. 1996. Early to mid Tertiary crustal extension in the Central Alps:

the Turba Mylonite Zone (Eastern Switzerland). *Tectonics*, **15**, 329–340.

OLSEN, K.H., BALDRIDGE, W.S. & CALLENDER, J.F. 1987. Rio Grande rift: an overview. *Tectonophysics*, **143**, 119–139.

PAQUET, J., FRANÇOIS, P. & NÉDÉLEC, A. 1981. Effect of partial melting on rock deformation: experimental and natural evidences on rocks of granitic compositions. *Tectonophysics*, **78**, 545–565.

PASSCHIER, C.W. & URAI, J.L. 1988. Vorticity and strain analysis using Mohr diagrams. *Journal of Structural Geology*, **10**, 755–763.

PATERSON, M.S. 1978. *Experimental Rock Deformation—the Brittle Field*. Springer, Berlin.

PATERSON, M.S. 1987. Problems in the extrapolation of laboratory rheological data. *Tectonophysics*, **133**, 33–43.

PATERSON, M.S. 1995. A theory for granular flow accommodated by material transfer via an intergranular fluid. *Tectonophysics*, **245**, 135–151.

PATERSON, M.S. 2001. A granular flow theory for the deformation of partially molten rock. *Tectonophysics*, in press.

PATERSON, S.R. & SCHMIDT, K.L. 1999. Is there a close spatial relationship between faults and plutons? *Journal of Strcutural Geology*, 8–9, **21**, 1131–1142.

PATERSON, S.R. & TOBISCH, A.T. 1992. Rates of processes in magmatic arcs: implications for the timing and nature of pluton emplacement and wall rock deformation. *Journal of Structural Geology*, **14**, 291–300.

PATERSON, S.R., VERNON, R.H. & TOBISCH, O.T. 1989. A review of criteria for the identification of magmatic and tectonic foliations in granitoids. *Journal of Structural Geology*, 3, **11**, 349–363.

PINARELLI, L., DEL MORO, A. & BORIANI, A. 1988. Rb–Sr geochronology of lower Permian plutonism in Massiccio dei Laghi, southern Alps (NW Italy). *Rendiconti Società Italiana di Mineralogia et Petrographia*, 2, **43**, 411–428.

PRICHARD, H.M., ALABASTER, T., HARRIS, N.B.W. & NEARY, C.R. (eds) 1993. *Magmatic Processes and Plate Tectonics*. Geological Society, London, Special Publications, **76**.

QUICK, J.E., SINIGOI, S. & MAYER, A. 1994. Emplacement dynamics of a large mafic intrusion in the lower crust, Ivrea–Verbano Zone, northern Italy. *Journal of Geophysical Research*, B11, **99**, 21559–21573.

RENNER, J., EVANS, B. & HIRTH, G. 2000. On the rheologically critical melt percentage. *Earth and Planetary Science Letters*, **181**, 585–594.

REY, P., BURG, J.P. & CARON, J.M. 1992. Middle and Late Carboniferous extension in the Variscan Belt: structural and petrological evidences from the Vosges massif (eastern France). *Geodinamica Acta*, **5**, 17–36.

RIVALENTI, G., ROSSI, A., SIENA, F. & SINIGOI, S. 1984. The Layered Series of the Ivrea–Verbano Igneous Complex, Western Alps, Italy. *Tschermaks Mineralogische und Petrographische Mitteilungen*, **33**, 77–99.

ROSENBERG, C.L. 2001. Deformation of partially molten granite: a review and comparison of experimental and natural case studies. *International Journal of Earth Sciences*, **90**, in press.

ROSENBERG, C.L. & HANDY, M.R. 2000. Syntectonic melt pathways during simple shearing of an anatectic rock analogue (norcamphor–benzamide). *Journal of Geophysical Research*, **105**, 3135–3149.

ROSENBERG, C.L. & HANDY, M.R. 2001. Melt migration during pure shear deformation of a partially molten rock analogue (norcamphor–benzamide). *Journal of Structural Geology*, in press.

ROSENBERG, C.L. & RILLER, U. 2000. Partial-melt topology in statically and dynamically recrystallized granite. *Geology*, **28**, 7–10.

ROSENBERG, C., BERGER, A. & SCHMID, S.M. 1995. Observations from the floor of a granitoid pluton: inferences on the driving force of final emplacement. *Geology*, **23**, 443–446.

RUBIN, A.M. 1998. Dike ascent in partially molten rock. *Journal of Geophysical Research*, B9, **103**, 20901–20919.

RUTTER, E.H. 1997. The influence of deformation on the extraction of crustal melts: a consideration of the role of melt-assisted granular flow. *In*: HOLNESS, M.B. (ed.) *Deformation-enhanced Fluid Transport in the Earth's Crust and Mantle*. Mineralogical Society Series, **8**, 82–110.

RUTTER, E.H. & MECKLENBURGH, J. 2001. The extraction of crustal melts from their protoliths and the flow behaviour of partially molten crustal rocks. *In*: BROWN, M. & RUSHMER, T. (eds) *Evolution and Differentiation of the Continental Crust*. Cambridge University Press, Cambridge.

RUTTER, E.H. & NEUMANN, D.H.K. 1995. Experimental deformation of partially molten Westerly granite under fluid-absent conditions, with implications for the extraction of granitic magmas. *Journal of Geophysical Research*, B8, **100**, 15697–15715.

RUTTER, E.H. & WHITE, S.H. 1979. The microstructures and rheology of fault gouges produced experimentally under wet and dry conditions at temperatures up to 400 °C. *Bulletin de Minéralogie*, 2–3, **102**, 101–109.

RUTTER, E.H., BRODIE, K.H. & EVANS, P.J. 1993. Structural geometry, lower crustal magmatic underplating and lithospheric stretching in the Ivrea–Verbano Zone, northern Italy. *Journal of Structural Geology*, **15**, 647–662.

SAWYER, E.W. 1991. Disequilibrium melting and the rate of melt–residuum separation during migmatization of mafic rocks from the Grenville Front, Quebec. *Journal of Petrology*, **32**, 701–738.

SAWYER, E.W. 1994. Melt segregation in the continental crust. *Geology*, **22**, 1019–1022.

SCHÄFER, A. & KORSCH, R.J. 1998. Formation and sediment fill of the Saar–Nahe Basin (Permo-

Carboniferous, Germany). *Zeitschrift der deutschen geologischen Gesellschaft*, 2, **149**, 233–269.

SCHEUBER, E. & REUTTER, K.J. 1992. Magmatic arc tectonics in the Central Andes between 21° and 25°S. *Tectonophysics*, **205**, 127–140.

SCHLUNEGGER, F. 1999. Controls of surface erosion on the evolution of the Alps: constraints from the stratigraphies of the adjacent foreland basins. *International Journal of Earth Sciences*, **88**, 285–304.

SCHMID, S.M. & HANDY, M.R. 1991. Towards a genetic classification of fault rocks: geological usage and tectonophysical implications. *In*: HSÜ, K.J., MACKENZIE, J. & MÜLLER, D. (eds) *Controversies in Modern Geology*. Academic Press, London, 339–361.

SCHMID, S.M., BOLAND, J.N. & PATERSON, M.S. 1977. Superplastic flow in fine grained limestone. *Tectonophysics*, **43**, 257–291.

SCHMID, S.M., PFIFFNER, O.A., FROITZHEIM, N., SCHÖNBORN, G. & KISSLING, E. 1996. Geophysical–geological transect and tectonic evolution of the Swiss–Italian Alps. *Tectonics*, **15**, 1036–1064.

SCHMID, S.M., RÜCK, P. & SCHREUERS, G. 1990. The significance of the Schams nappes for the reconstruction of the paleotectonic and orogenic evolution of the Penninic zone along the NFP-20 traverse (Grisons, eastern Switzerland). *Mémoire de la Société Géologique de France*, **156**, 263–287.

SCHOLZ, C.H. 1990. Mechanics of faulting. *Annual Review of Earth and Planetary Sciences*, **17**, 309–334.

SCHOLZ, C.H. 1998. Earthquakes and friction laws. *Nature*, **391**, 37–42.

SCHÖNBORN, G. & SCHUMACHER, M.E. 1994. Controls on thrust tectonics along basement–cover detachment. *Schweizerische Mineralogische und Petrographische Mitteilungen*, **74**, 421–436.

SECOR, D.T. 1965. Role of fluid pressure in jointing. *American Journal of Science*, **263**, 633–646.

SHAW, H.R. 1980. Fracture mechanisms of magma transport from the surface. *In*: HARGRAVES, R.B. (ed.) *Physics of Magmatic Processes*. Princeton University Press, Princeton, NJ, 201–264.

SIBSON, R.H. 1977. Fault rocks and fault mechanisms. *Journal of the Geological Society, London*, **133**, 191–213.

SIBSON, R.H. 1985. A note on fault reactivation. *Journal of Structural Geology*, **7**, 751–754.

SIBSON, R.H. 1986. Earthquakes and rock deformation in crustal fault zones. *Annual Review of Earth and Planetary Sciences*, **14**, 149–175.

SINGH, J. & JOHANNES, W. 1996. Dehydration melting of tonalites. Part I. Beginning of melting. *Contributions to Mineralogy and Petrology*, **125**, 16–25.

SINIGOI, S., QUICK, J., CLEMENS-KNOTT, D., MAYER, A. & DEMARCHI, G. 1994. Chemical evolution of a large mafic intrusion in the lower crust, Ivrea–Verbano Zone. *Journal of Geophysical Research*, B11, **99**, 21575–21590.

SMITH, J.V. 1997. Shear thickening dilatancy in crystal-rich flows. *Journal of Volcanological and Geothermal Research*, **79**, 1–8.

SNOKE, A.W., KALAKAY, T.J., QUICK, J.E. & SINIGOI, S. 1999. Development of a deep-crustal shear zone in response to syntectonic intrusion of mafic magma into the lower crust, Ivrea–Verbano zone, Italy. *Earth and Planetary Science Letters*, **166**, 31–45.

SPEER, J.A., MCSWEEN, H.Y. JR & GATES, A.E. 1994. Generation, segregation, ascent, and emplacement of Alleghanian plutons in the southern Appalachians. *Journal of Geology*, **102**, 249–267.

STREIT, J.E. 1997. Low frictional strength of upper crustal faults: a model. *Journal of Geophysical Research*, B11, **102**, 24619–24626.

TALBOT, C.J. 1999. Can field data constrain rock viscosities? *Journal of Structural Geology*, **21**, 949–958.

TROMMSDORFF, V. & CONNOLLY, J.A.D. 1996. The ultramafic contact aureole about the Bregaglia (Bergell) tonalite: isograds and a thermal model. *Schweizerische Mineralogische und Petrographische Mitteilungen*, **76**, 537–548.

TROMMSDORFF, V. & NIEVERGELT, P. 1983. The Bregaglia Iorio intrusive and its field relations. *Memorie della Società Geologica Italiana*, **26**, 55–68.

VAN DER MOLEN, I. & PATERSON, M.S. 1979. Experimental deformation of partially-melted granite. *Contributions to Mineralogy and Petrology*, **70**, 299–318.

VAUCHEZ, A. & EGYDIO DA SILVA, M. 1992. Termination of a continental-scale strike-slip fault in partially melted crust: the West Pernambuco shear zone, northeast Brazil. *Geology*, **20**, 1007–1010.

VIGNERESSE, J.L. 1995. Control of granite emplacement by regional deformation. *Tectonophysics*, **249**, 173–186.

VIGNERESSE, J.L., BARBEY, P. & CUNEY, M. 1996. Rheological transitions during partial melting and crystallization with application to felsic magma segregation and transfer. *Journal of Petrology*, **37**, 1579–1600.

VON BLANCKENBURG, F. & DAVIES, J.H. 1995. Slab breakoff: a model for syncollisional magmatism and tectonics in the Alps. *Tectonics*, **14**, 120–131.

WEERTMAN, J. 1968. Dislocation climb theory of steady state creep. *American Society of Metallurgy Transactions*, **61**, 681–694.

WICKHAM, S.M. 1987. The segregation and emplacement of granitic magmas. *Journal of the Geological Society, London*, **144**, 281–297.

ZHANG, S., COX, S.F. & PATERSON, M.S. 1994. The influence of room temperature deformation on porosity and permeability in calcite aggregates. *Journal of Geophysical Research*, **99**, 15761–15775.